Winter School on
«Membranes and Membrane Reactors»

FROM MEMBRANE DISTILLATION TO MEMBRANE CRYSTALLIZATION: FUNDAMENTALS AND APPLICATIONS

Efrem Curcio
Department of Environmental Engineering, University of Calabria (Italy)
e.curcio@unical.it

UNIVERSITÀ DELLA CALABRIA

1Cube Office (Microlab), Eindhoven (NL), 27-28 January 2025

MEMBRANE CONTACTORS

- MEMBRANE DISTILLATION
- OSMOTIC DISTILLATION
- MEMBRANE CRYSTALLIZATION
- GAS-LIQUID MEMBRANE CONTACTOR
- MEMBRANE EMULSIFICATION
- SUPPORTED LIQUID MEMBRANES

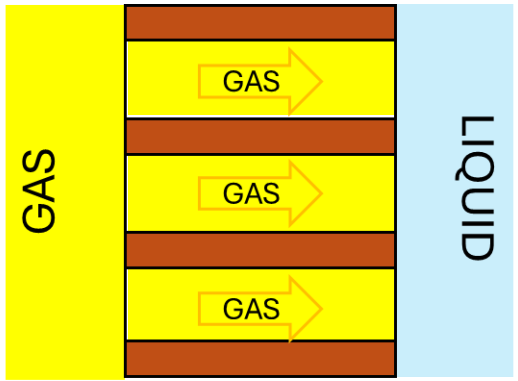

G-L equilibrium (Henry's Law)

$$p_i = \frac{c_i}{H}$$

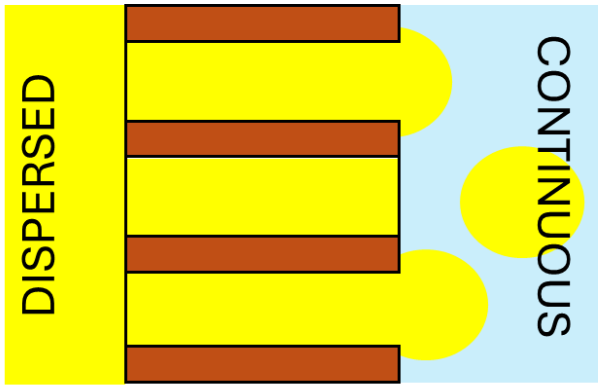

Pressure gradient ΔP

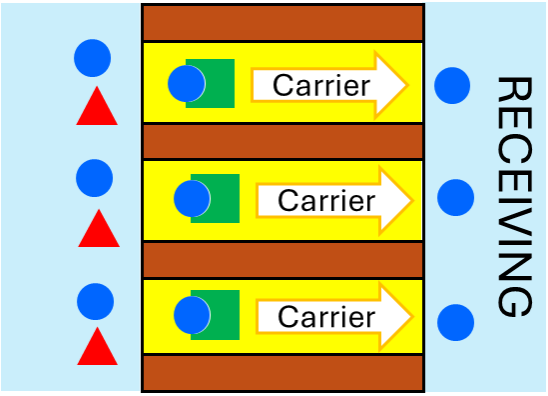

Facilitated transport

MEMBRANE CONTACTORS are systems employed to "keep in contact" two phases. The membrane does not offer any selectivity for a specific component, but simply sustains an interface where physical and/or chemical equilibrium takes place.

DRIVING FORCE IN MEMBRANE DISTILLATION

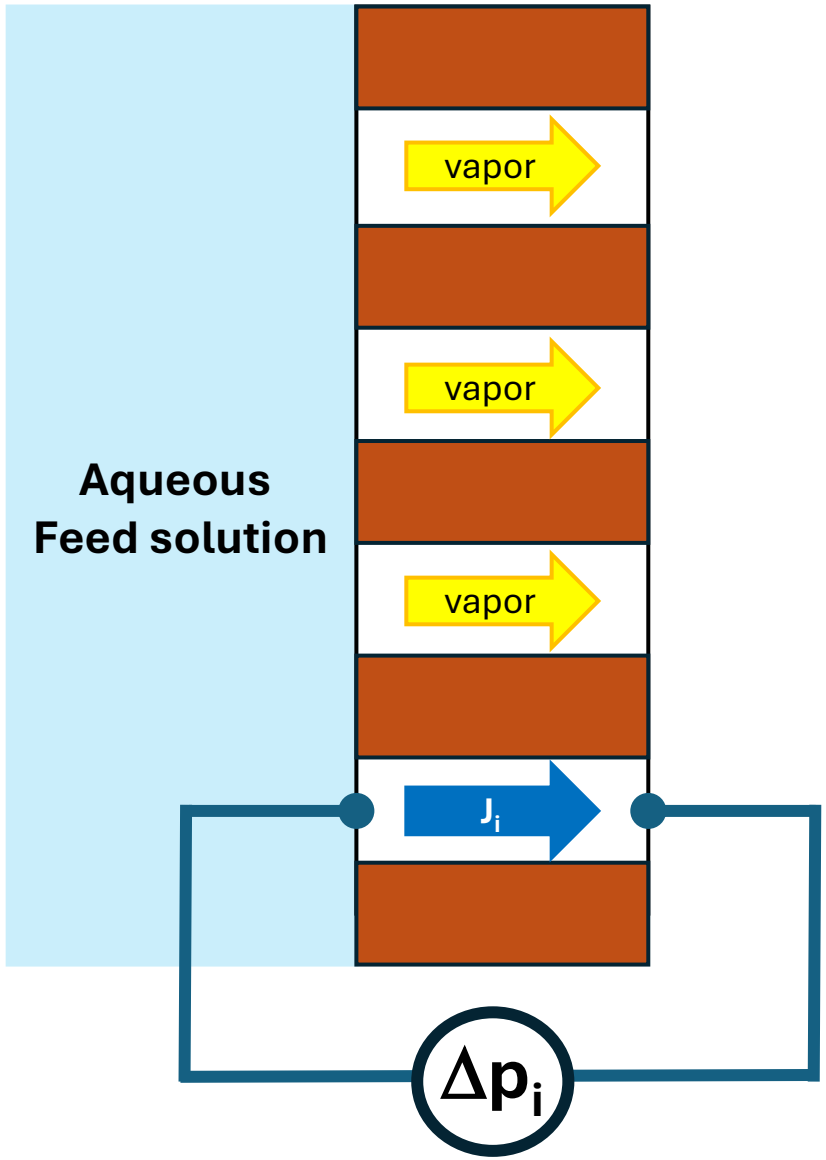

Volatile components (typically water) evaporate at the interface of a microporous hydrophobic membrane and diffuse across the membrane

Transmembrane flux: J_i

Driving force: difference of partial pressure at the membrane interface Δp_i

RAOULT'S LAW

$$p_i = p_i^0 a_i = p_i^0 x_i \gamma_i$$

partial pressure

vapour pressure

activity

molar fraction

activity coefficient

Difference of Vapor Pressure ⇔ **Temperature**

MEMBRANE DISTILLATION

The vapour pressure of a pure substance varies with temperature according to the Clausius-Clapeyron equation:

$$\frac{dp^0}{dT} = \frac{p^0 \lambda}{RT^2}$$

λ: latent heat of vaporization
(=9.7 cal/mole for water at 100°C)

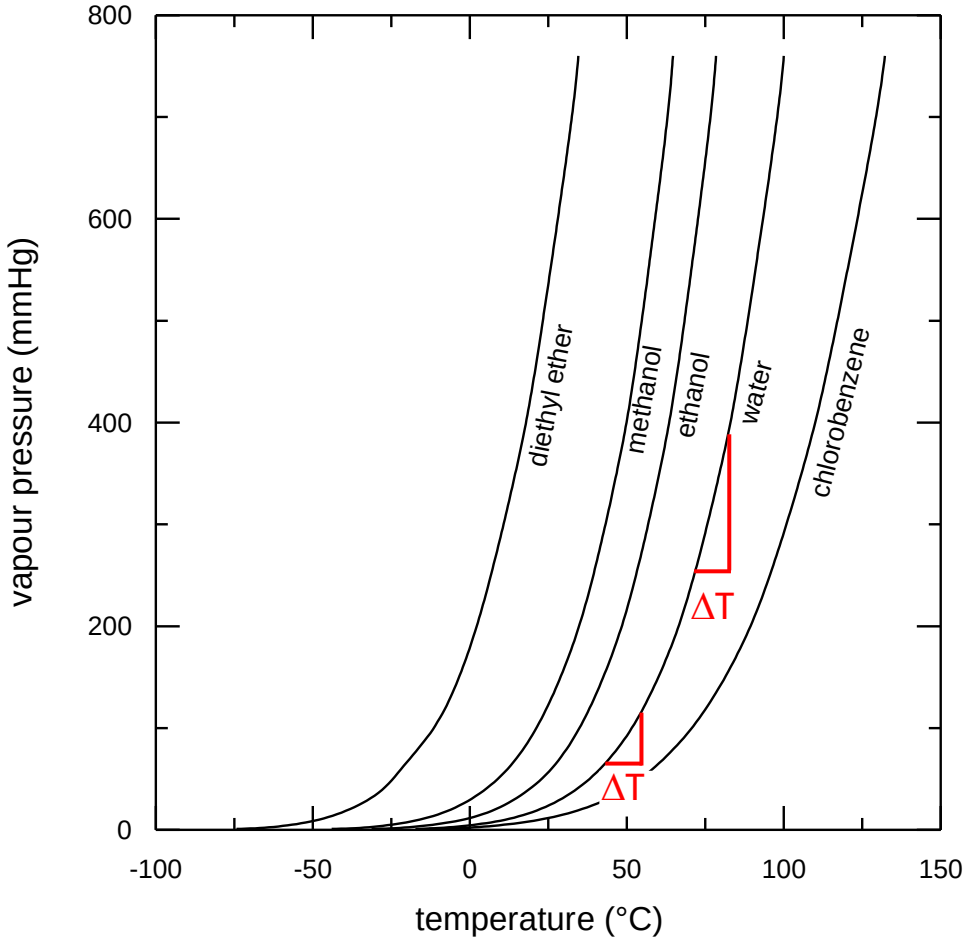

Difference of Partial Pressure

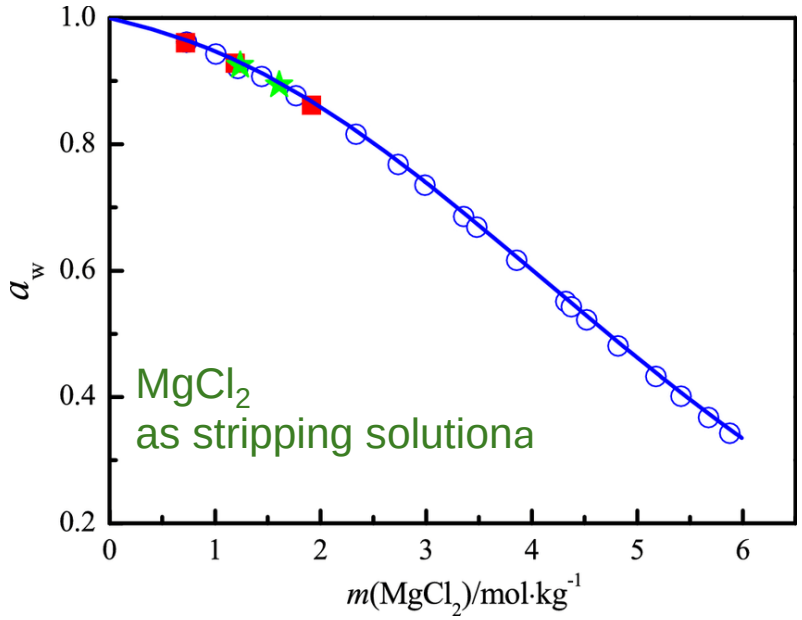

Difference of Activity ⇔ **Concentration**

OSMOTIC DISTILLATION

MEMBRANE DISTILLATION vs REVERSE OSMOSIS

Seawater

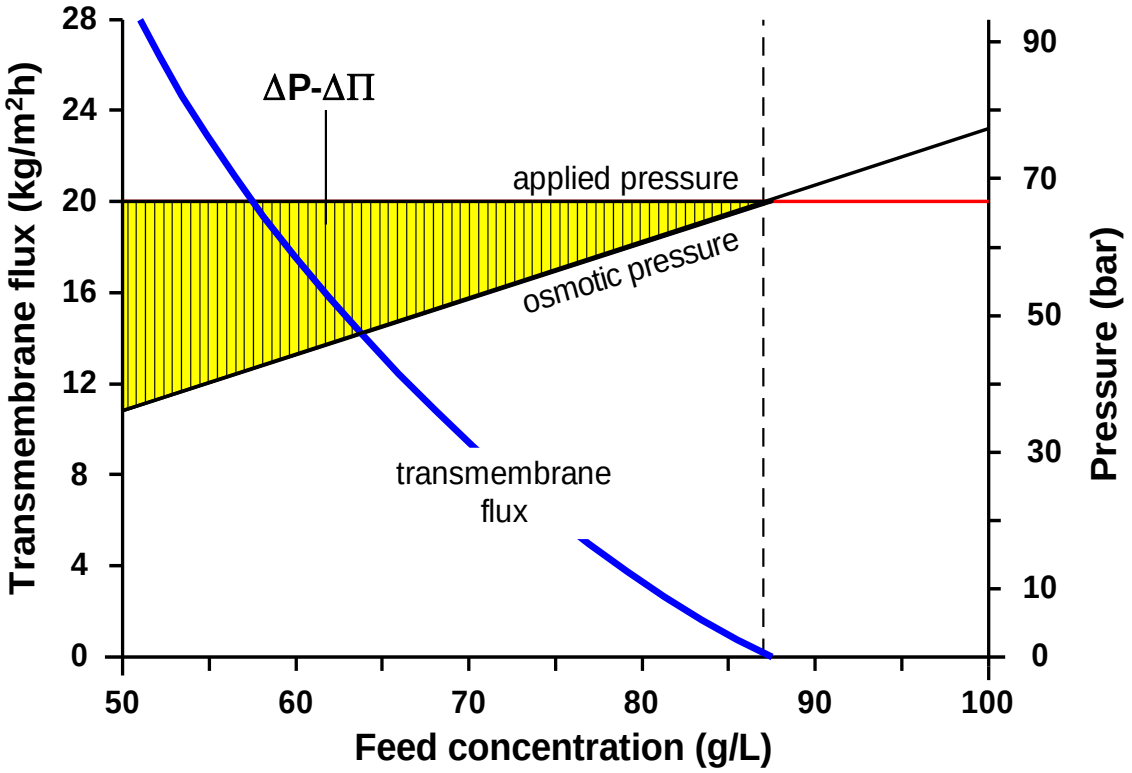

RO: sharp decrease of driving force due to osmotic and concentration polarization phenomena at higher solute concentration.

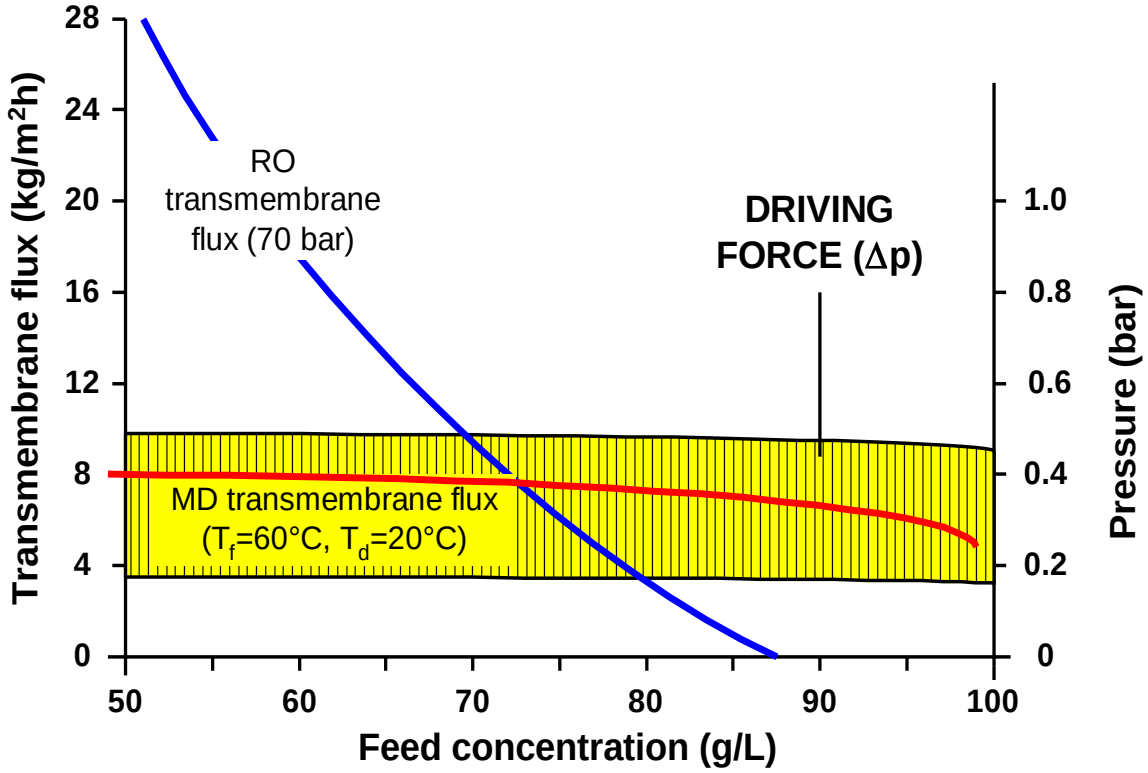

MD: low sensitivity of driving force (vapor pressure difference) to solute concentration and consequent ability to achieve high recovery.

PRO

- Very high rejection of non-volatile solutes such as macromolecules, colloidal species, ions etc.
- Low sensitivity to osmotic and concentration polarization phenomena: possibility to reach high recovery factor
- Moderate working temperatures (50-80°C)
- Possibility to reuse efficiently low-grade or waste heat streams, as well as alternative energy sources (solar, wind or geothermal)

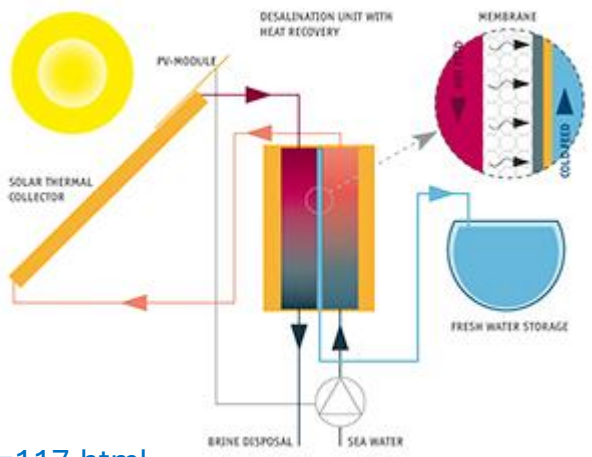

https://www.mediras.eu/index.php@id=117.html

- Reduction of corrosion problems due to the possibility to use plastic equipment

CONTRA

- Higher energy consumption with respect to pressure-driven membrane processes (estimated that the energy requirement in MD is about 120–1700 kWh/m^3 compared to 2.5–7.0 kWh/m^3 for the RO process)
- Energy efficiency limited by temperature polarization
- Only a restricted class of polymeric materials (inherently hydrophobic) offers a sufficient chemical resistance and operational stability
- Risk of wetting in presence of surfactants (e.g. humic acid)

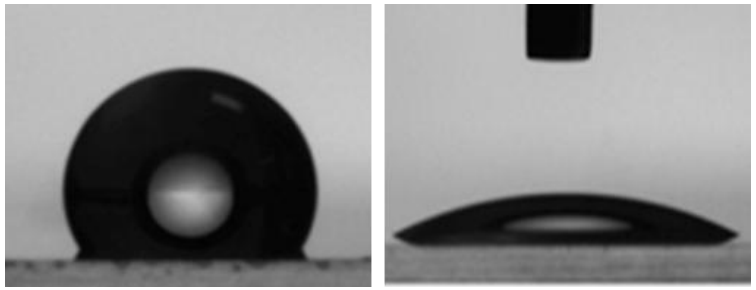

BASIC MD CONFIGURATIONS

Depending on the method adopted to reduce the partial pressure of the transported component on the distillate side, MD is classified in four basic configurations:

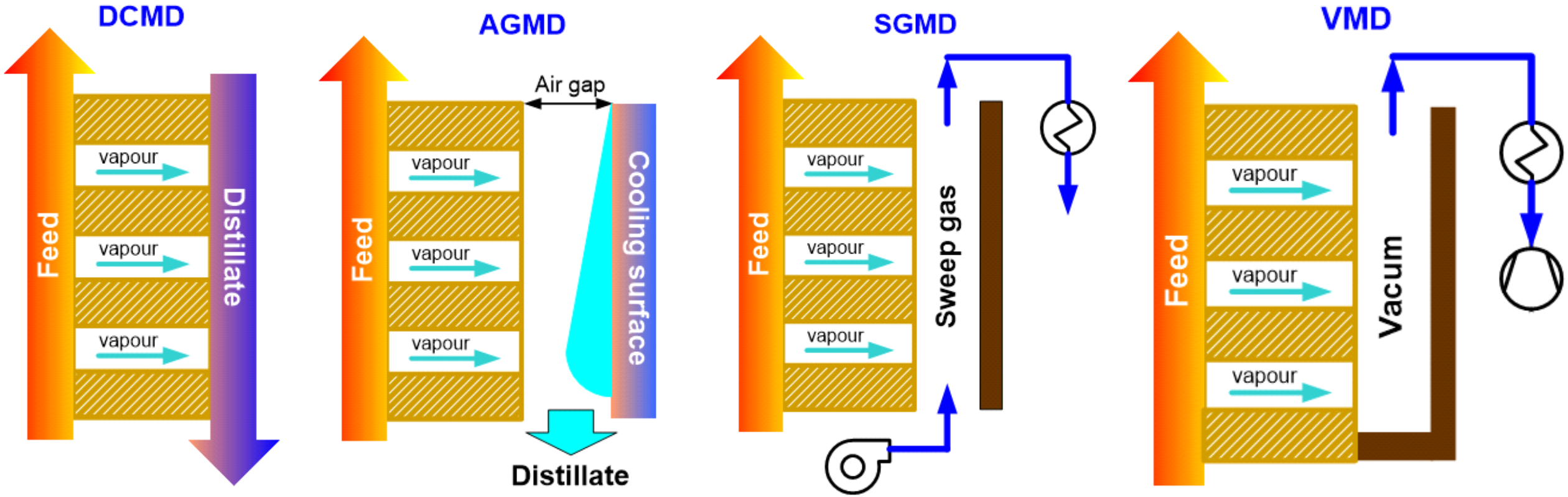

Distillate in liquid phase contacting the membrane and set at a lower temperature with respect to feed

Distillate compartment consisting of a thin and stagnant air gap and a condensing cold surface

Distillate compartment flushed with an inert sweep gas which collects vapor molecules, whereas their condensation takes place in a subsequent step

Vacuum applied at the distillate side at a level below the saturation pressure of water at the feed temperature, whereas the vapor is condensed in a subsequent step

Advantages and disadvantages of the different MD configurations

MD configuration	Advantages	Drawbacks
DCMD	- Technologically simple in design, easy scale-up - Moderate transmembrane flux - Direct condensation of the distillate inside the module	- High thermal conductive loss
AGMD	- Low thermal conductive loss - Feed solution used as cooling medium (pre-heating) - Direct condensation of the distillate inside the module (heat recovery)	- Low transmembrane flux due to additional mass transfer resistance of the air gap
SGMD	- Moderate transmembrane flux - Low thermal conductive loss	- High cost for condensing the distillate
VMD	- High transmembrane flux - Very low thermal conductive loss	- High cost for vacuum - High cost for condensing the distillate - Higher risk of wetting

CIRCULAR WATER TECHNOLOGIES

CWT operates under a license from Scarab Development AB

Air Gap MD

https://circularwatertechnologies.com/

MEMSYS WATER TECHNOLOGIES GMBH

https://www.memsys.eu/

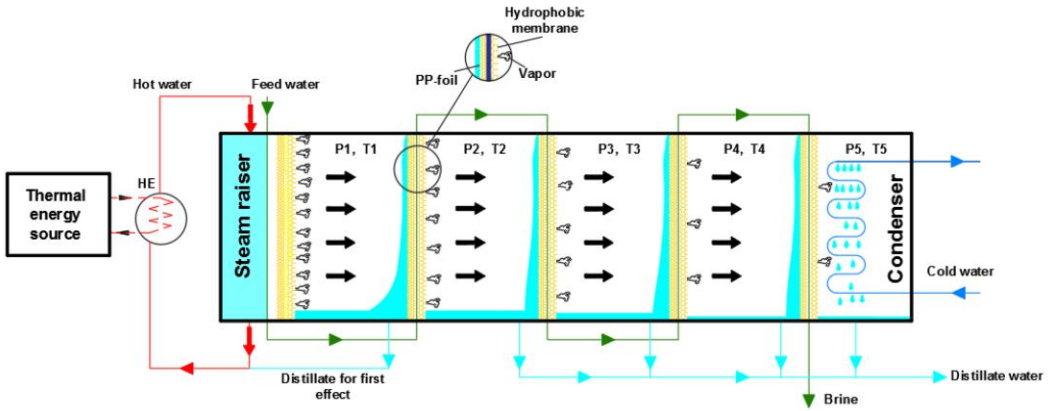

Vacuum Multi Effect Membrane Distillation (V-MEMD) modules

MEMSIFT INNOVATIONS PTE LTD

Hollow Fibers MD

https://memsift.com/products/

AQUASTILL

https://www.aquastill.nl/

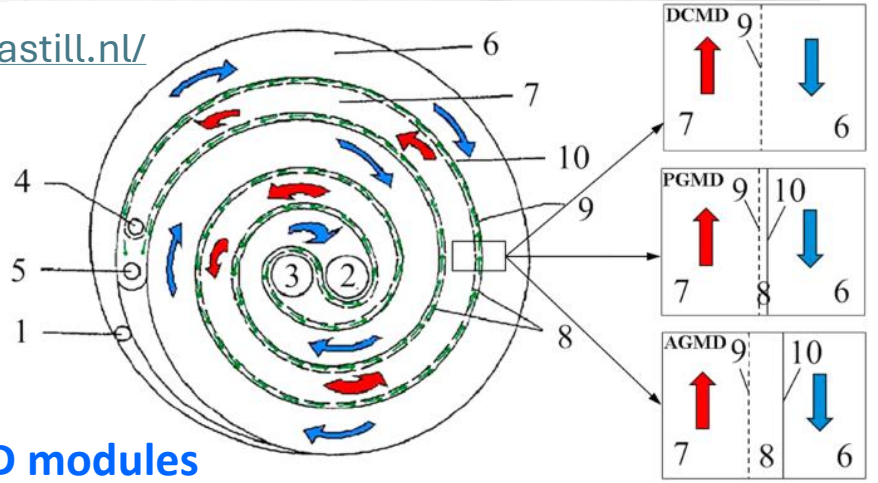

Spiral Wound MD modules

MEMBRANES FOR MEMBRANE DISTILLATION

- hydrophobic/non-wetting (to retain the liquid phase)
- microporous (for optimal vapor transport rate)

https://doi.org/10.1016/j.desal.2016.04.006
https://doi.org/10.1016/j.memsci.2014.09.016
DOI: 10.1002/adfm.202301549

Polymer	Structure	Surface energy ($*10^{-3}$ N m^{-1})	Avg Thermal conductivity W m^{-1} K^{-1}	Commercially available membranes
PVDF	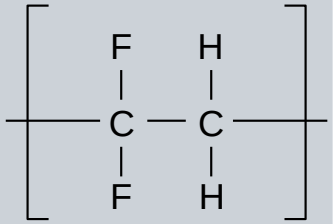	30.3	0.2	Millipore GVHP (d_{av} = 0.22 μm, δ = 110 μm, ε = 75%, LEP = 105 kPa) Millipore HVHP (d_{av} = 0.45 μm, δ = 140 μm, ε = 75%, LEP = 204 kPa)
PTFE	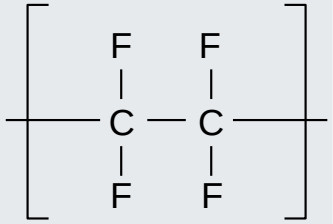	9–20	0.27	Gelman TF200 (d_{av} = 0.2 μm, δ = 178 μm, ε = 80%, LEP = 282 kPa)
PP	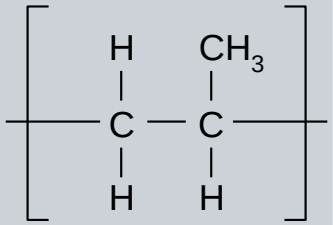	30	0.21	Accurel PP (d_{av} = 0.2 μm, δ = 91 μm, ε = –, LEP = –)

Contact angle	Liquid entry pressure	Porosity	Pore diameter	Thickness
> 90°	> 2.0 bar	>70%	0.1–0.8 µm	100-150 µm

PVDF

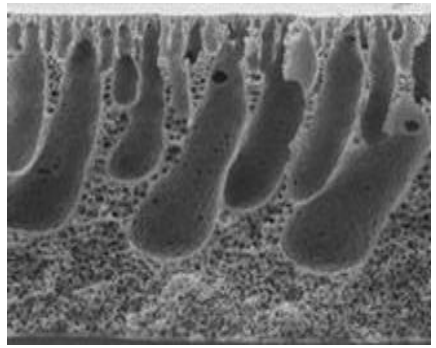

Non Solvent Induced Phase Separation (NIPS)

Dissolved in dipolar aprotic, high boiling point solvents (NMP, DMA, DMF)
Pore formers: LiCl, PVP, PEG

PTFE

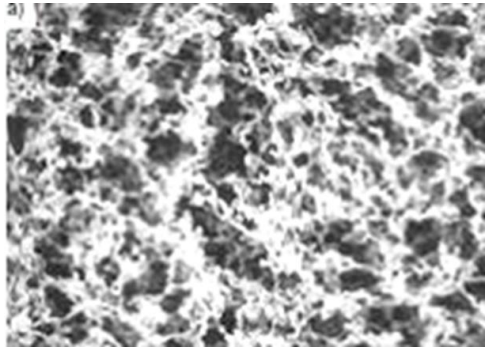

Sintering

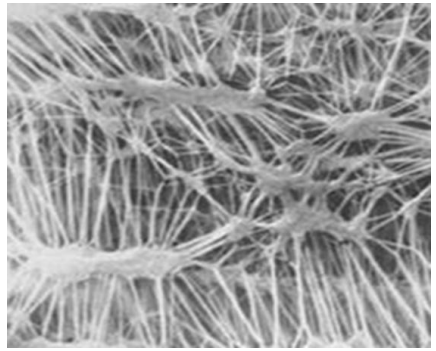

Stretching

Processability challenges due to reluctance of non-polar polymers to most solvents

PP

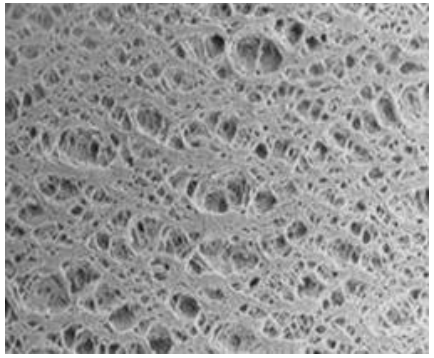

Temperature Induced Phase Separation (TIPS)

Dissolved in non-polar solvents (e.g. Xylene, Decalin) at elevated temperature

LIQUID ENTRY PRESSURE

YOUNG-LAPLACE EQUATION

$$\Delta P_{entry} = -\frac{2\Theta\,\gamma_{LG}\cos\theta}{r_{p,\max}}$$

γ_{LG}: liquid surface energy

Θ: geometric factor related to the pore structure (= 1 for cylindrical pores)

θ: contact angle

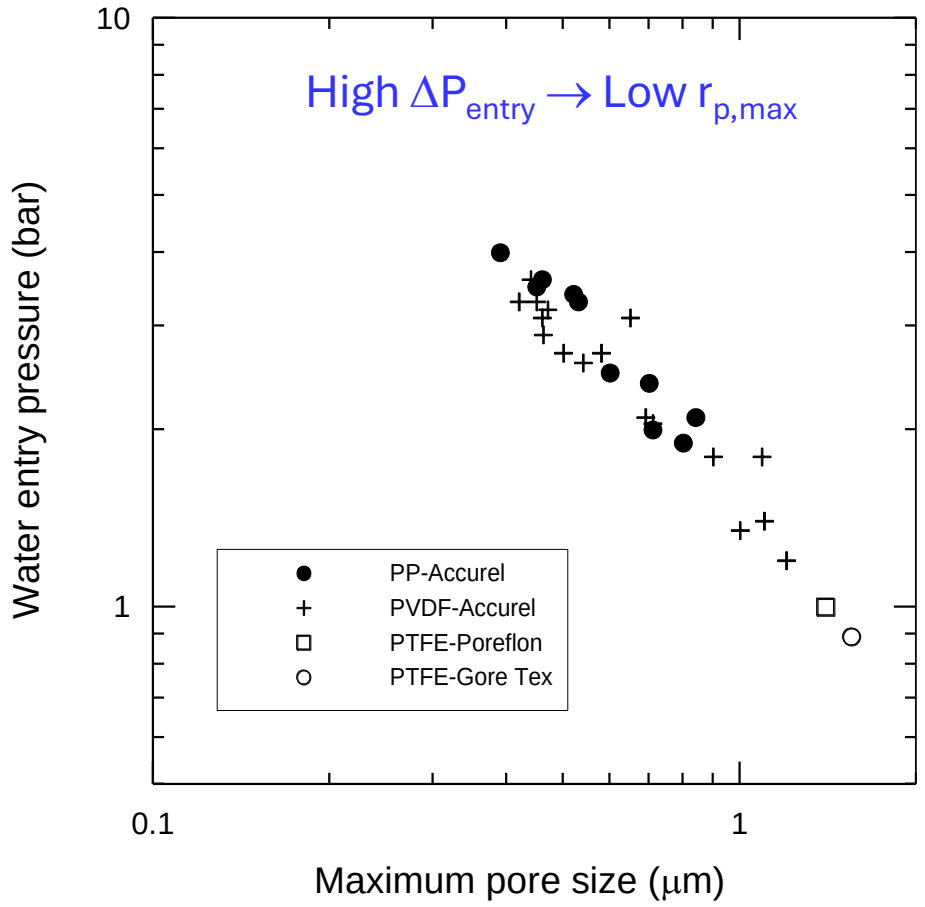

Water pressure entry for different membranes as a function of the maximum pore size

K. Schneider, W. Holz, R. Wollbeck, J. Membrane Sci. 39 (1988) 25-42

YOUNG EQUATION

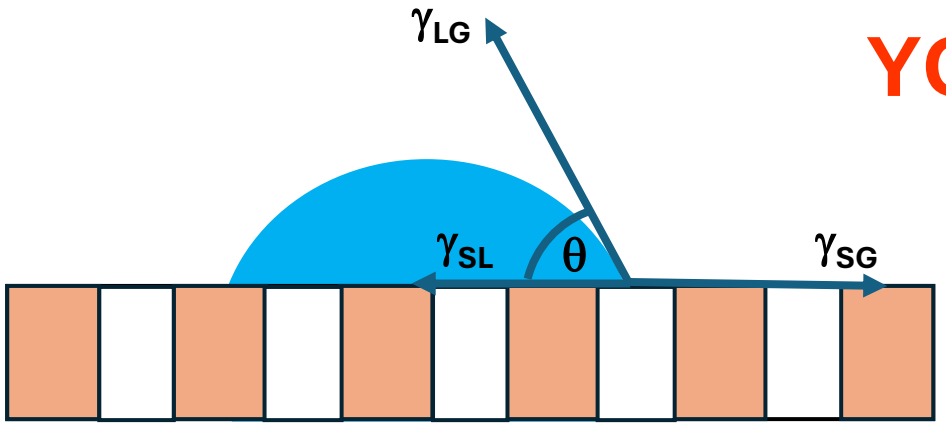

$$\gamma_{LG}\cos\theta + \gamma_{SL} = \gamma_{SG}$$

or

$$-\gamma_{LG}\cos\theta = \gamma_{SL} - \gamma_{SG}$$

High

High

Low

Mechanical equilibrium
at triple point C

γ_{LG}: *liquid surface tension*
γ_{SG}. *solid surface tension*
γ_{SL}: *solid-liquid surface tension*

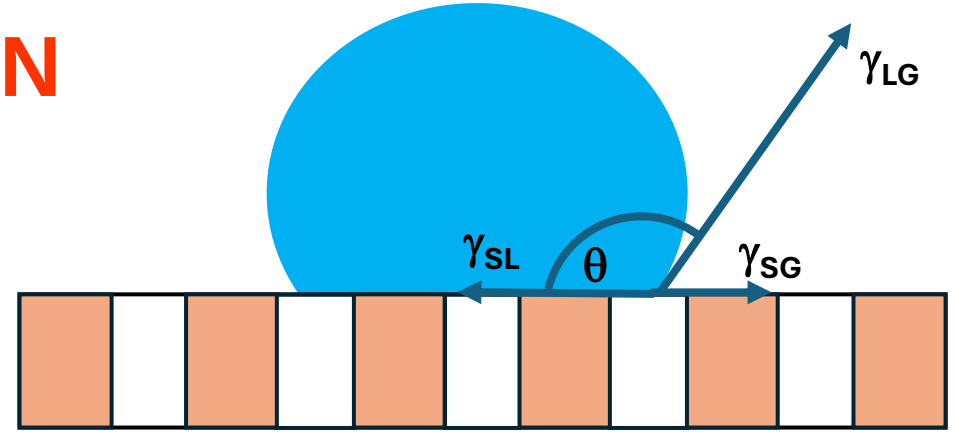

Test liquid	γ_{LG} (mJ/m)
Water	72
Glycerol	64
Ethylene glycol	48
Formamide	58
Diiodomethane	50.8
Dimethylsulfoxide	44
Chloroform	27.2

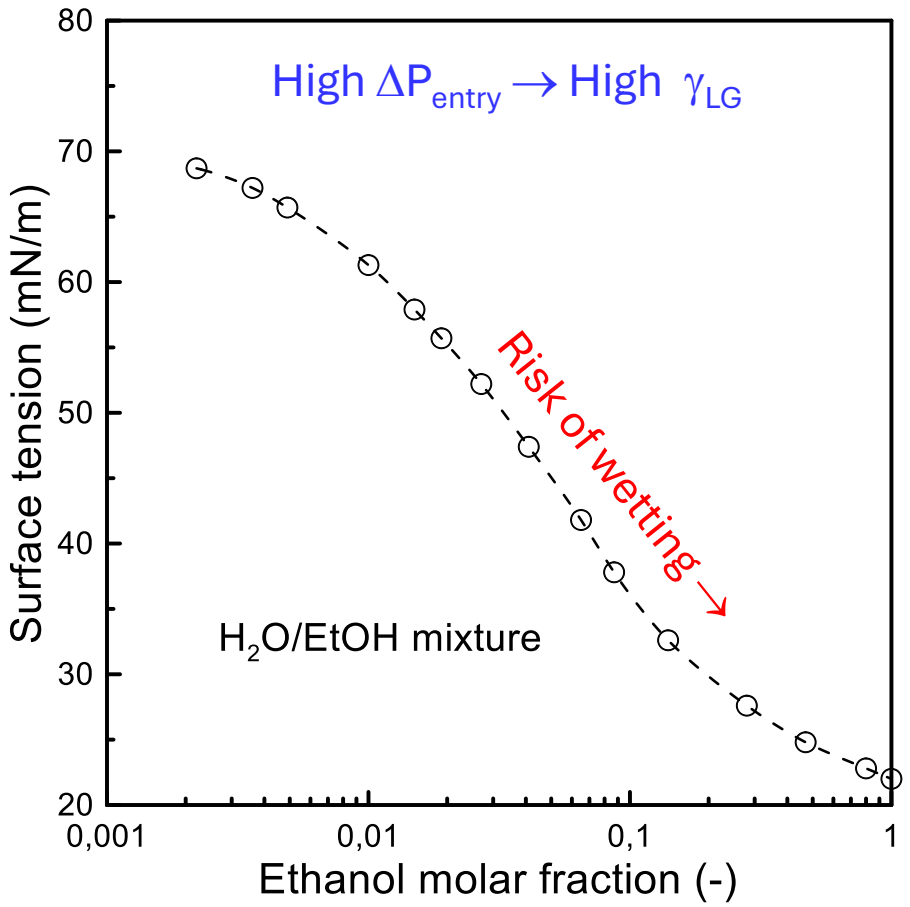

ENHANCING MEMBRANE STABILITY

REDUCING SENSITIVITY TO FOULING

- Casting, spraycoating, electrospinning hydrophilic polymers

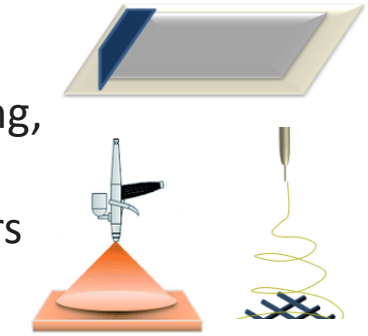

- Casting PVA hydrogel

- Plasma-induced graft polymerization of hydrophylic monomers (e.g. acrylic acid), zwitterions …

ENHANCING HYDROPHOBICITY

- Direct membrane functionalization via tetrafluoromethane (CF4) plasma modification

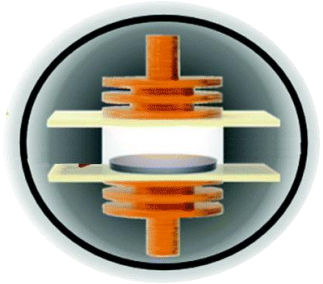

- Surface texture: use NPs functionalized with fluorinated compounds to increase roughness (Wenzel, Cassie-Baxter)

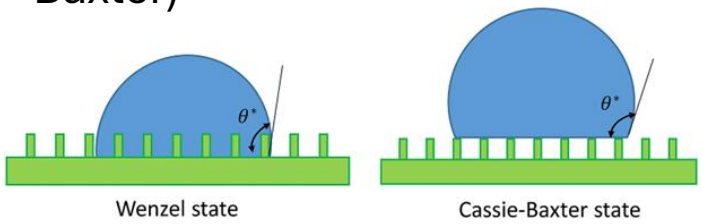

OMNIPHOBICITY

- [Ar, air, N_2] plasma-activated grafting of hydrophobic fluoroalkylsilane (FAS)

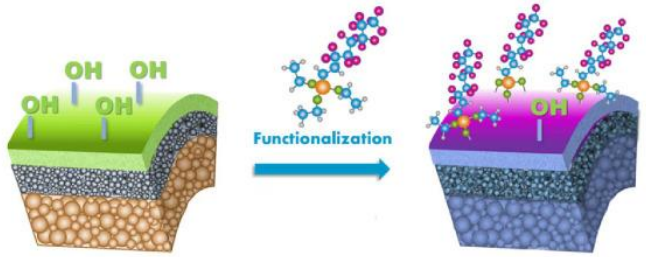

MASS TRANSFER IN MEMBRANE DISTILLATION

Mass transport for MD process can be conveniently described in terms of serial resistances upon the transfer between the bulks of two phases contacting the membrane

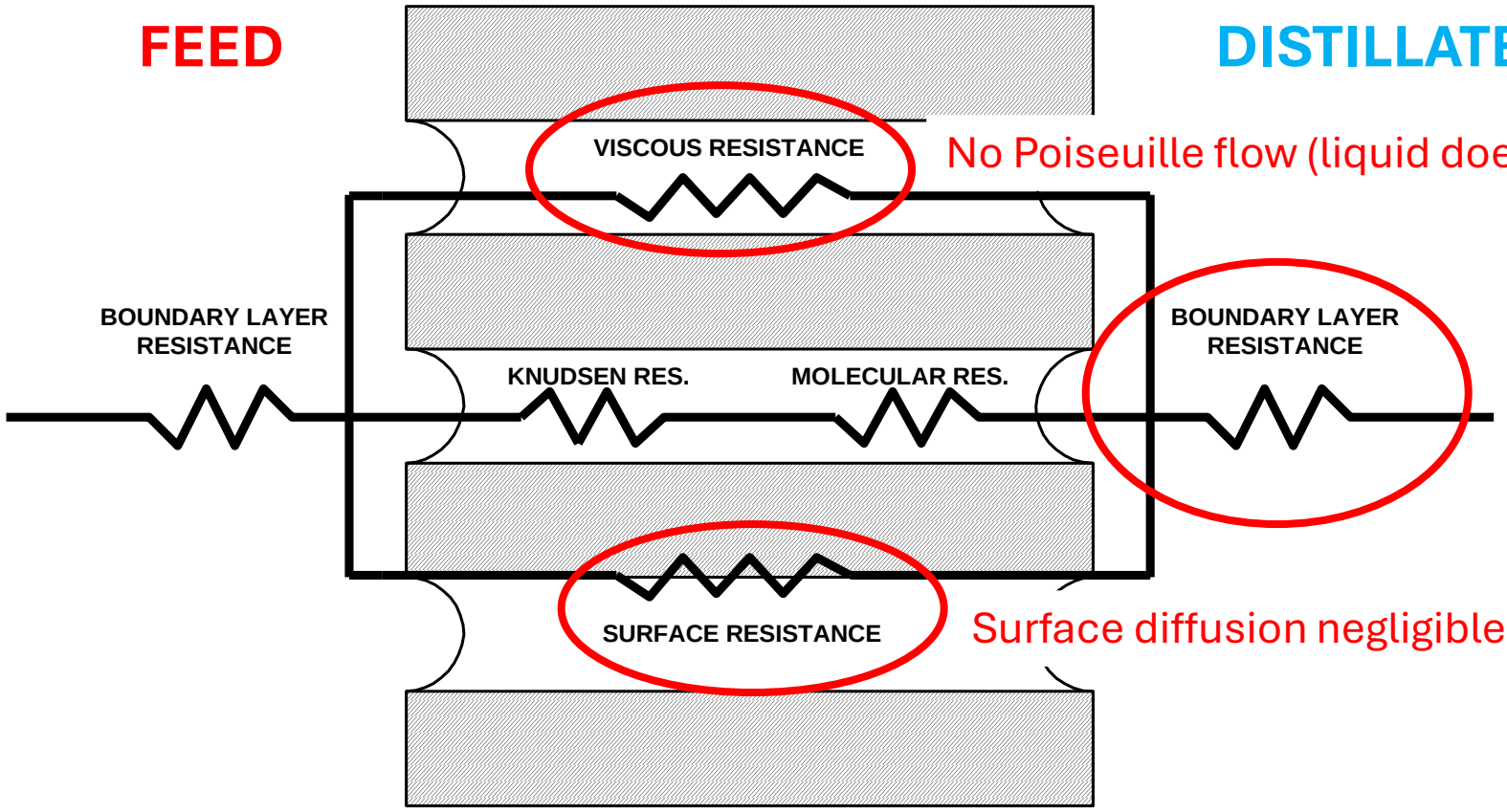

MASS TRANSFER WITHIN THE POROUS MEMBRANE

KNUDSEN NUMBER (Kn) = $\dfrac{\text{mean free path } \iota \text{ of diffusing molecules}}{\text{mean pore size of the membrane}}$

Kn>1

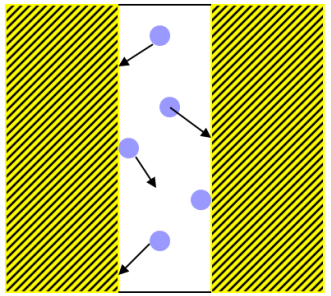

$$D_{ie}^{k} = \frac{2\varepsilon r}{3\tau}\sqrt{\frac{8RT}{\pi M_i}}$$

KNUDSEN DIFFUSION
Predominance of collisions between molecules and membrane walls

MEAN FREE PATH FOR AIR-WATER VAPOR MIXTURE

$$\iota_{a/w} = \frac{k_B \bar{T}}{\pi\left(\left(\sigma_w + \sigma_a\right)/2\right)^2 P}\frac{1}{\sqrt{1+\left(M_w/M_a\right)}}$$

For an average temperature = 60°C, the mean free path of water in air is 0.11 μm

Coexhistence of Knudsen Diffusion and Molecular Diffusion

Kn<1

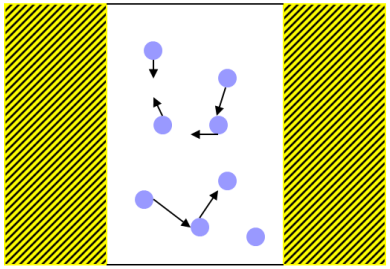

$$D_{ije}^{0} = \frac{\varepsilon}{\tau} P D_{ij}^{0}$$

Negligible in VMD (pores are de-airated)

MOLECULAR DIFFUSION
Predominance of collisions between molecules

DUSTY GAS MODEL

$$\frac{J_i}{D_{ie}^{k}} + \sum_{j=1\neq i}^{n}\frac{p_j J_i - p_i J_j}{D_{ij}^{e}} = -\frac{\nabla p_i}{RT}$$

p: partial pressure
P: total pressure
M: molecular weight
r: pore radius
ε: porosity
τ: tortuosity
J: transmembrane diffusive flux

BOUNDARY LAYER RESISTANCE

When solvent molecules are transferred through the membrane, the retained solute tends to accumulate at the membrane surface where its concentration gradually increases.

CONCENTRATION POLARIZATION (negative impact on **activity** of the evaporating compound)

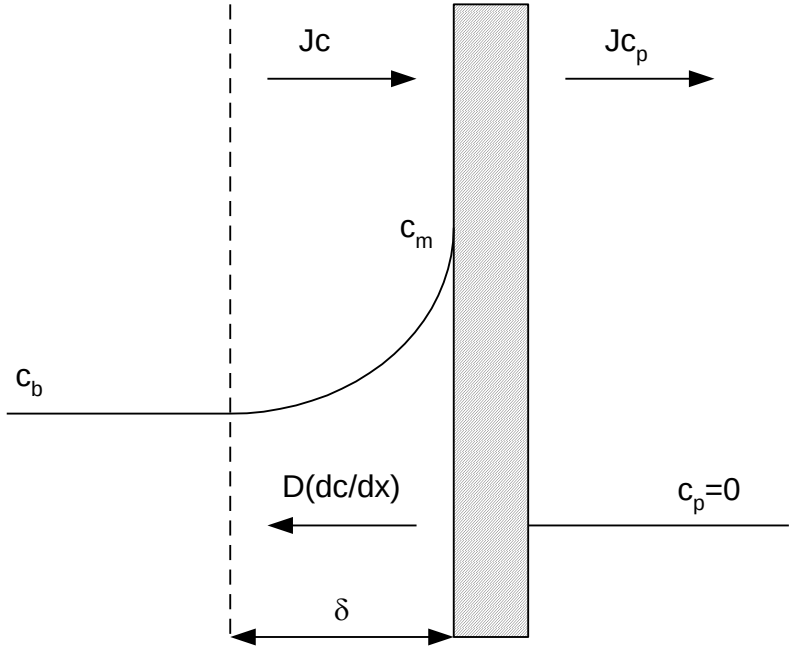

$$J = k_x \ln \frac{c_m}{c_b}$$

Mass transfer coefficient

Empirical expressions based on dimensionless numbers are generally used:

Dittus-Boelter equation

$$Sh = \alpha \, \mathrm{Re}^{\beta} \, Sc^{\gamma}$$

Sh, Sherwood number $$Sh = \frac{k_x d_h}{D}$$

(d_h: hydraulic diameter, D: diffusion coefficient)

Re, Reynolds number $$\mathrm{Re} = \frac{\rho \, v \, d_h}{\mu}$$

(ρ: fluid density, v: fluid velocity, μ: fluid viscosity)

Sc, Schmidt number $$Sc = \frac{\mu}{\rho \, D}$$

Examples of specific predictive equations for mass transfer coefficients in MD

Correlation	α	β	γ	k_x(10^{-5} m/s)	Comment	Reference
$k_x=\beta Q^{\gamma}$	-	**$4.02\cdot10^{-5}$**	**0.38**	**3.5 – 7.6**	Stirred cell Q: volumetric feed flowrate (L/min)	S. Bandini, C. Gostoli, G.C. Sarti, J. Membrane Sci., 73 (1992) 217-229
$Sh=\alpha\,\mathrm{Re}^{\beta}\,Sc^{\gamma}$	**2.0**	**0.48**	**0.33**	-	Stirred cell Stirring rate: 200-800 rpm	M. Sudoh, K. Takuwa, H. Iizuka, K. Nagamatsuya. J. Membrane Sci., 131 (1997) 1-7
	1.86	**0.38**	**0.38**	-	Hollow fibres	M. Tomaszewska, M. Gryta, A.W. Morawski, J. Membrane Sci., 102 (1995) 113-122
	0.96-0.45φ	**0.55**	**0.33**	**17.5**	Helicoidal hollow fibres ϕ: angle of inclination	M.J. Costello, P.A. Hogan and A.G. Fane, Proc. Euromembrane '97, 23-27 Jun 1997, The Netherlands
	0.023	**0.33**	**0.33**	**6.6-7.4**	Tubular fibres	K.W. Lawson and D.R. Lloyd. J. Membrane Sci., 120 (1996) 111-121

HEAT TRANSFER IN MEMBRANE DISTILLATION

occurring simultaneously with mass transfer

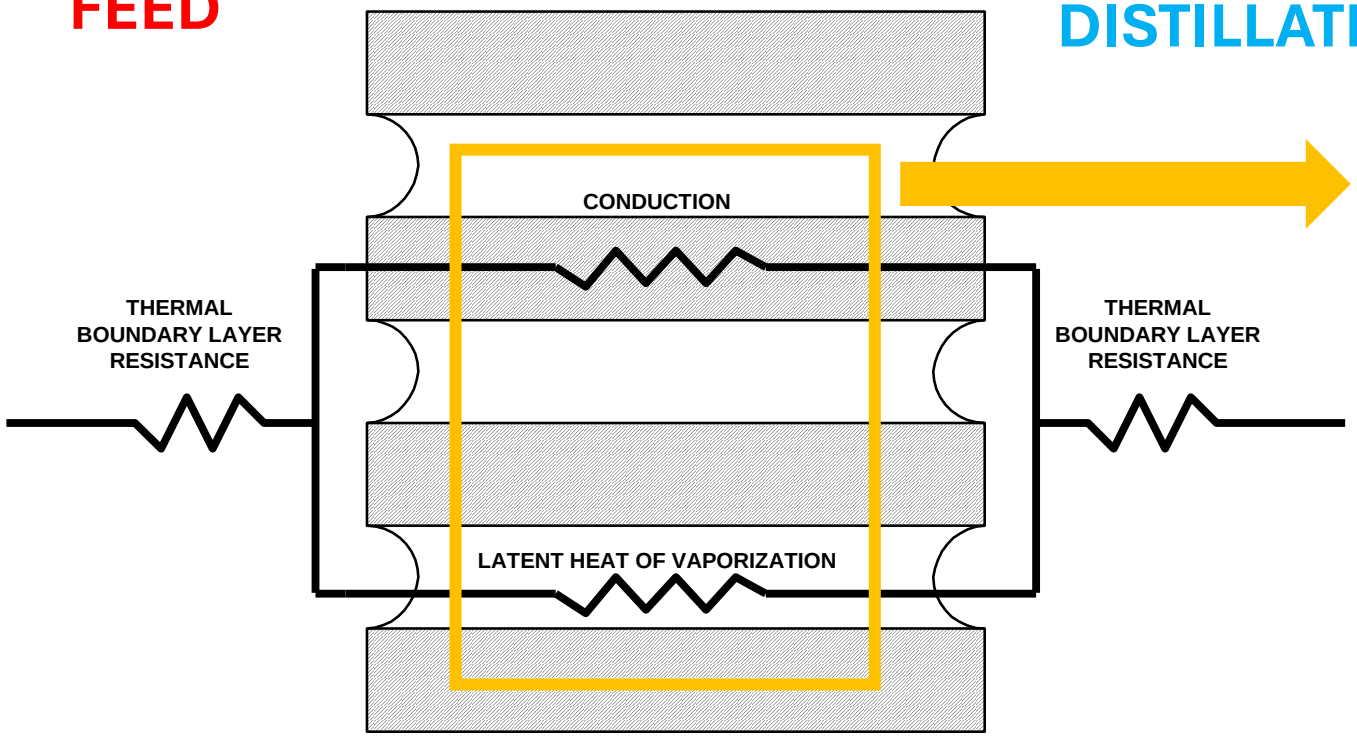

Heat flux across the membrane (W/m^2)

$$q_m = -k_m \frac{\Delta T}{\delta_m} + J_i \lambda$$

$\Delta T = (T_m^f - T_m^d)$

k_m: Membrane thermal conductivity

δ_m: Membrane thickness

λ: Latent heat

$$k_m = (1-\varepsilon)k_s + \varepsilon k_g$$

ε: porosity

$$k_{air} = 2.72 \cdot 10^{-3} T + 7.77 \cdot 10^{-5} T$$

$$q_f = h_f (T_\infty^f - T_m^f)$$

$$q_d = h_d (T_m^d - T_\infty^d)$$

Heat transfer coefficient

Heat flux $q = h\,\Delta T$

(W/m^2)

Nu, Nusselt number

$$Nu = \frac{h\,D}{k}$$

Gr, Grashof number

$$Gr = \frac{D^3 \rho^2 g \beta \Delta T}{\mu^2}$$

Pr, Prandtl

$$\mathrm{Pr} = \frac{c_p\,\mu}{k}$$

Gz, Graetz number

$$Gz = \frac{\dot{m}\,c_p}{k\,L}$$

Equation	Comments
$Nu = 0.13\,\mathrm{Re}^{0.64}\,\mathrm{Pr}^{0.38}$	Laminar flow
$Nu = 0.097\,\mathrm{Re}^{0.73}\,\mathrm{Pr}^{0.13}$	Laminar flow
$Nu = 1.62\left(\mathrm{Re}\,\mathrm{Pr}\left(\frac{d}{L}\right)\right)^{0.33}$	Laminar flow, tangential flux
$Nu = 0.023\,\mathrm{Re}^{0.8}\,\mathrm{Pr}^{0.33}\left(\frac{\mu}{\mu_w}\right)^{0.14}$	Turbulent liquid
$Nu = 3.66 + \frac{0.067\,Gz}{1 + 0.04\,Gz^{0.66}}$	Laminar flow, VMD
$Nu = 0.036\,\mathrm{Re}^{0.8}\,\mathrm{Pr}^{0.33}\left(\frac{d}{L}\right)^{0.055}$	Turbulent flow

BOUNDARY LAYER RESISTANCE: TEMPERATURE POLARIZATION

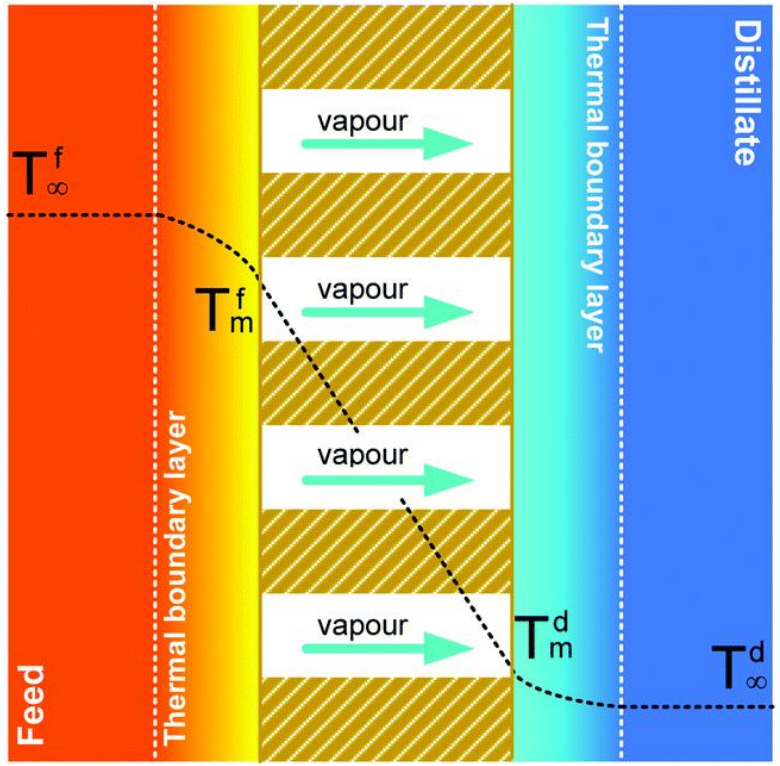

Direct Contact Membrane Distillation

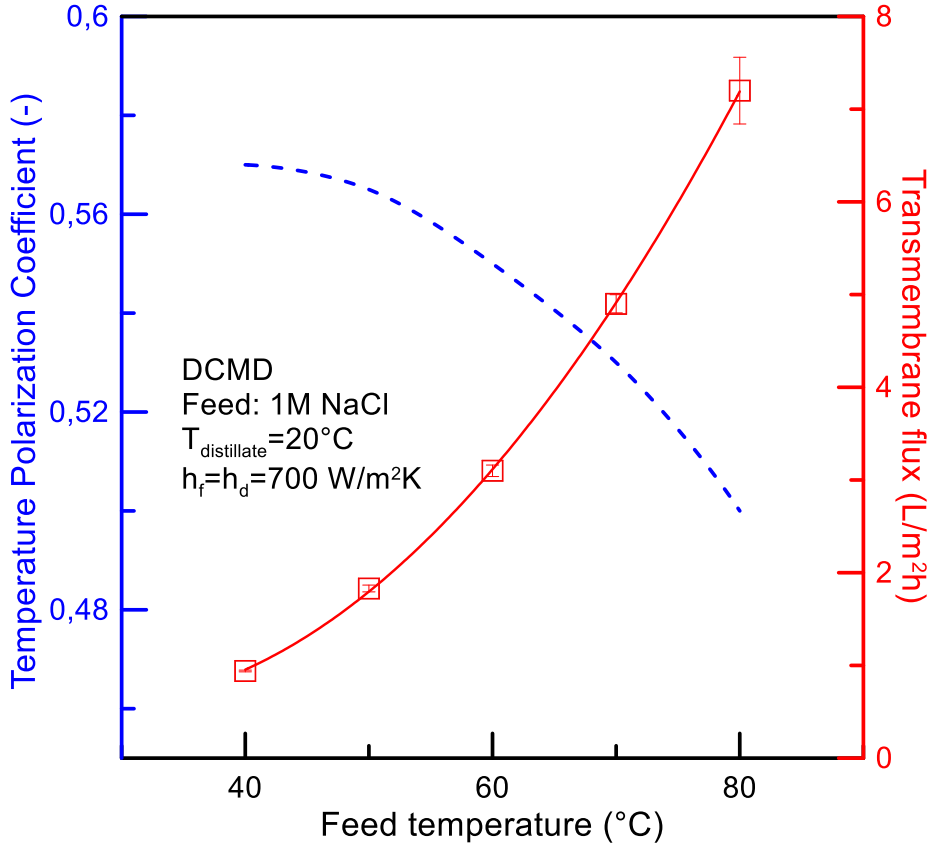

- Temperature polarization (TP) intrinsically related to the removal of latent heat associated with water evaporation
- TP is quantified by the temperature polarization coefficient (TPC):

$$TPC = \frac{T_m^f - T_m^d}{T_\infty^f - T_\infty^d}$$

- TP decreases the thermal efficiency of MD operation

PHOTOTHERMAL MEMBRANE DISTILLATION (PhMD)

Photothermal nanoparticles can **efficiently release heat under optical excitation**. The electromagnetic field strongly drives mobile electrons, and the energy gained turns into heat.

Heat generation is enhanced in regime of ***plasmon resonance*** involving a collective motion of a large number of electrons.

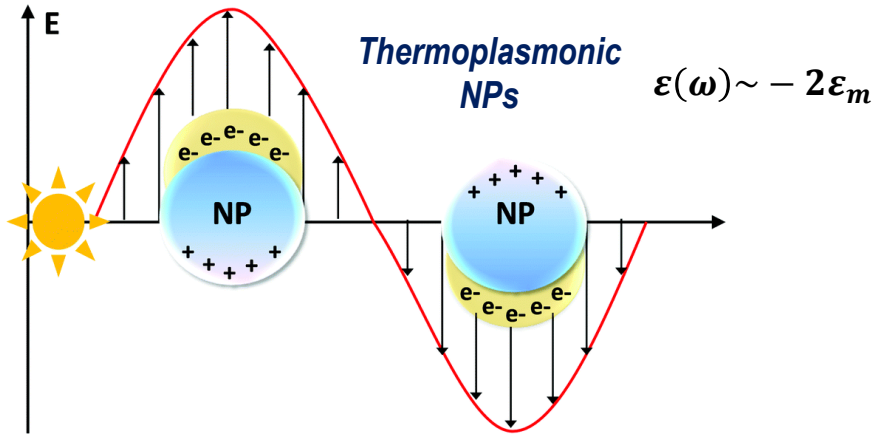

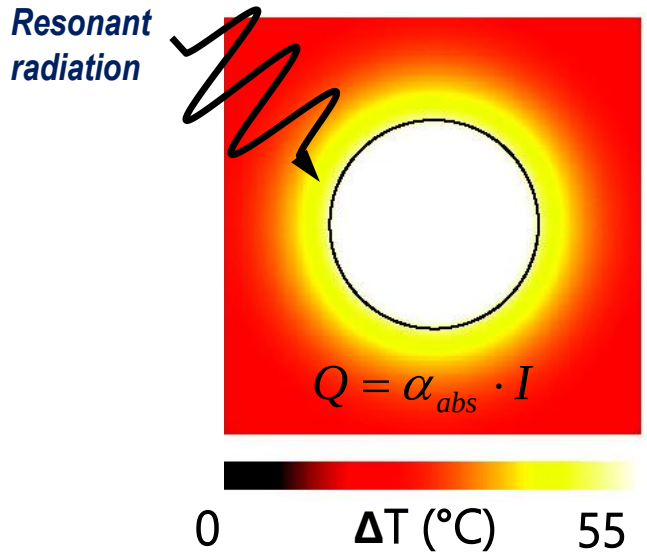

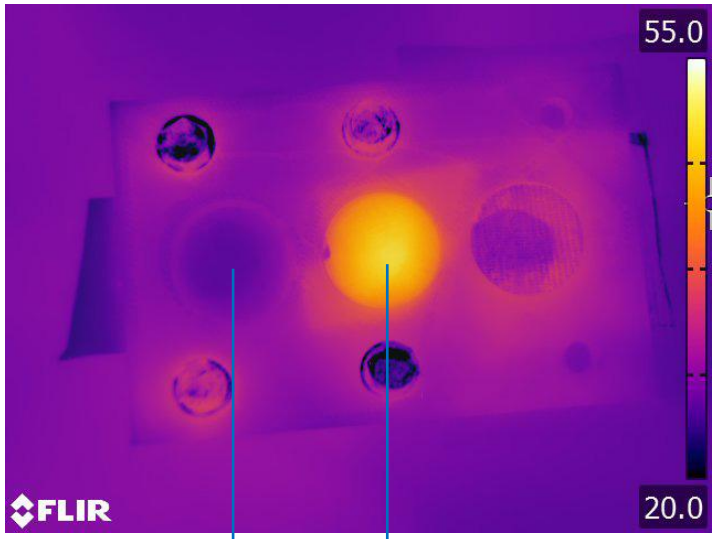

S. Santoro, A. H. Avci,a A. Politano, E. Curcio. The advent of thermoplasmonic membrane distillation. Chem. Soc. Rev. 2022,51, 6087

The immobilization of photothermal NPs in a membrane guarantee high light-to-heat conversion

THE FIRST STEP: PhMD VIA Ag NPs

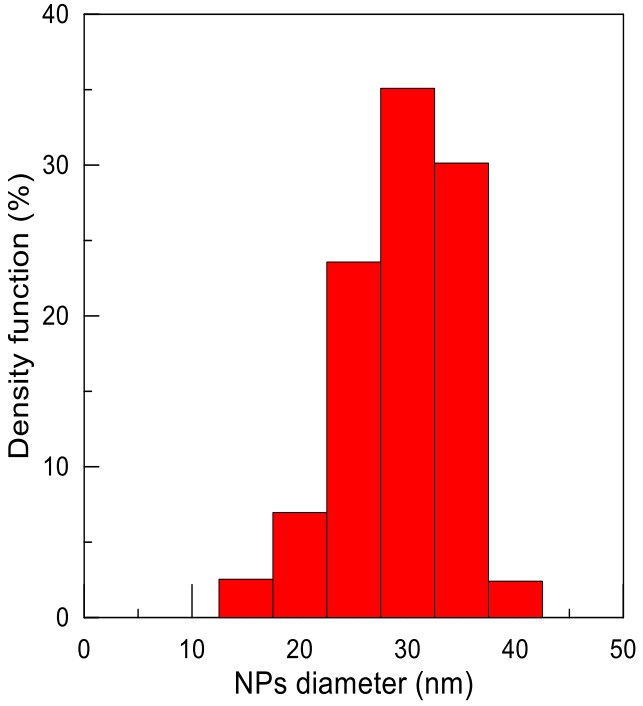

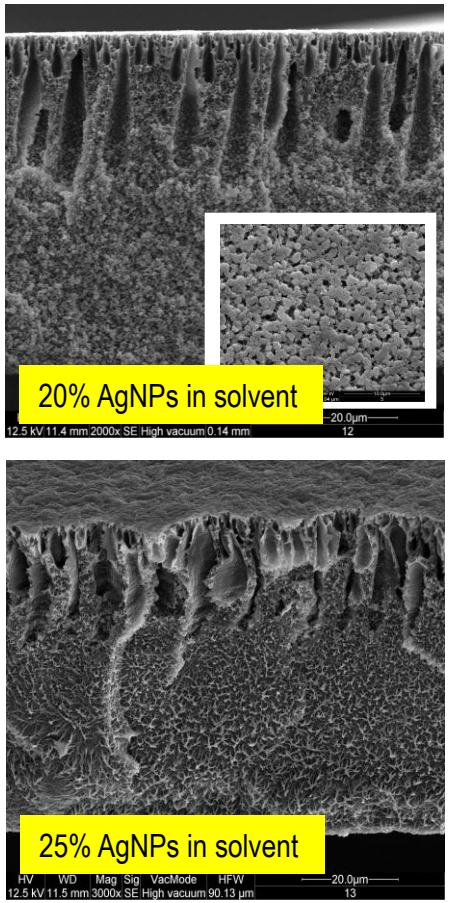

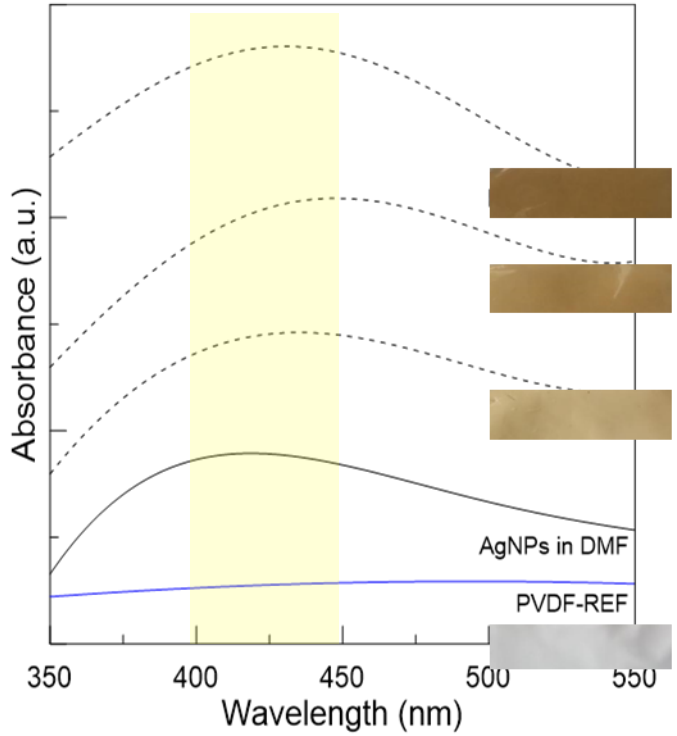

- Ag NPs with **average diameter of 31 ± 4 nm** dispersed in microporous PVDF membrane
- Maximum absorbance intensity around 420 nm, corresponding to the wavelength of the plasmon resonance of Ag NPs

A. Politano, P. Argurio, G. Di Profio, V. Sanna, A. Cupolillo, S. Chakraborty, H. A. Arafat, E. Curcio. Photothermal Membrane Distillation for Seawater Desalination. Advanced Materials 29/2 (2017) 1603504

PhMD VIA Ag NPs UNDER UV RADIATION

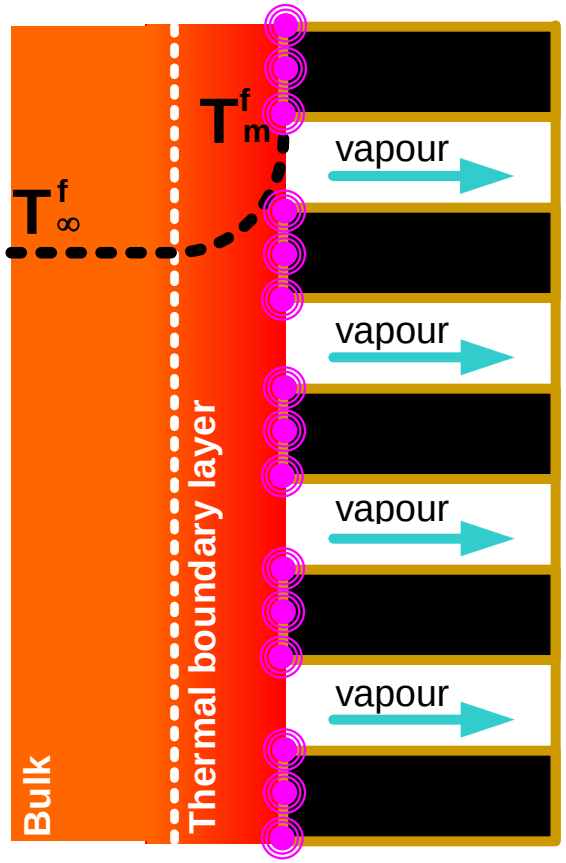

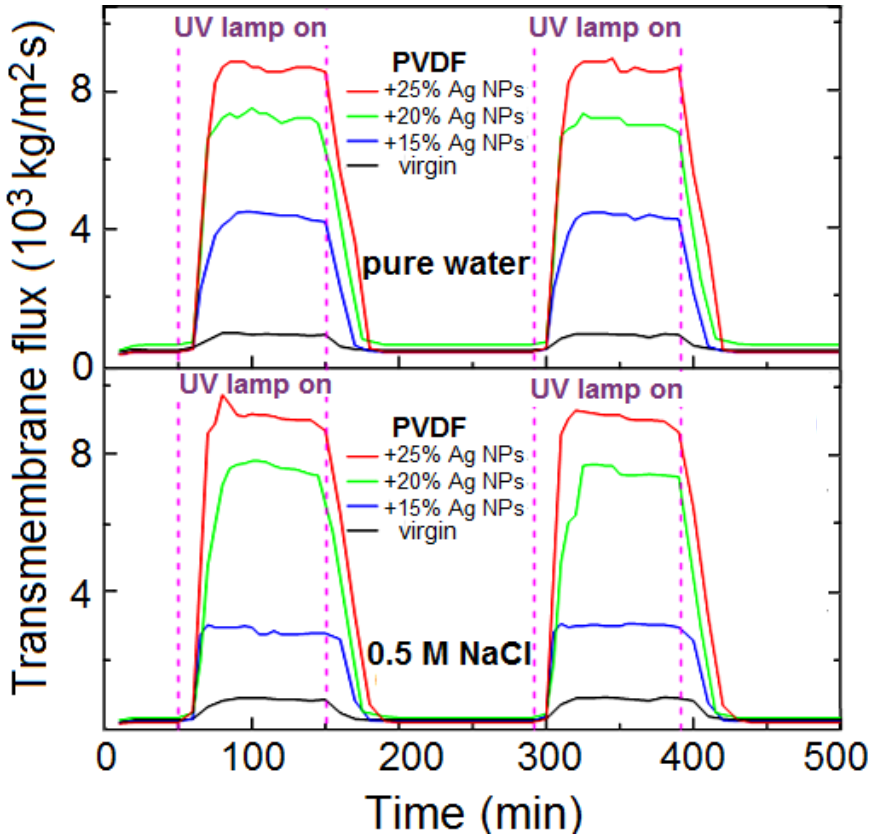

- Measured fluxes to pure water and 0.5M NaCl solution up to 9- and 11-fold higher than the corresponding values for unloaded PVDF membranes, respectively
- Photothermal effect activated by UV radiation, insufficient photothermal efficacy in the visible
- High cost of Ag-based membrane

FROM UV TO SOLAR RADIATION: NiSe AND CoSe TOPOLOGICAL NODAL LINE SEMIMETALS

Electronic band structure

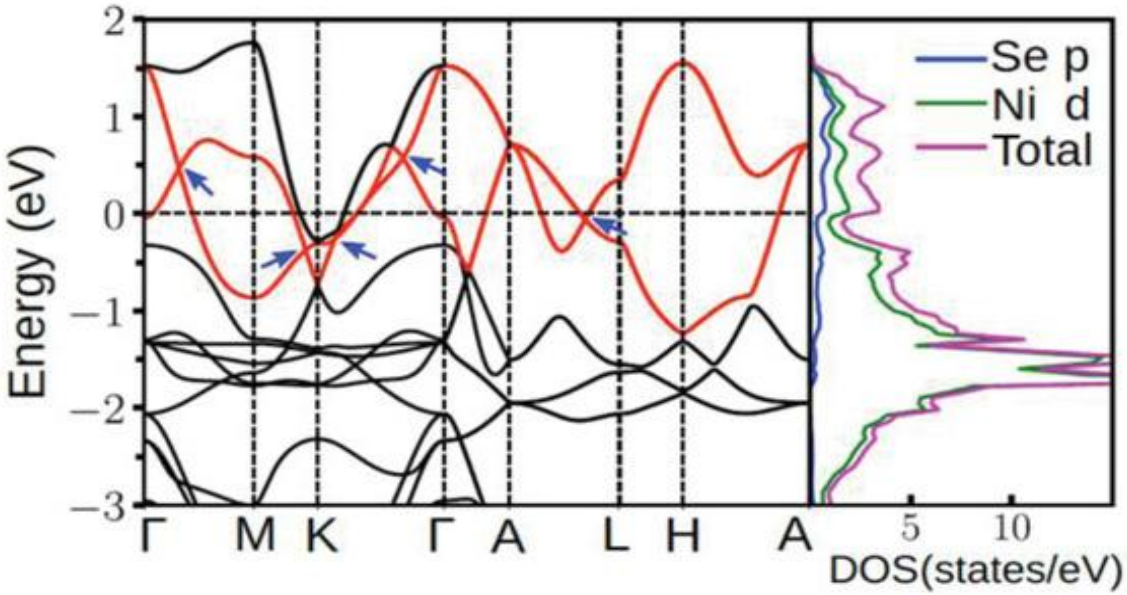

the number of different states at a particular energy level that electrons are allowed to occupy

Topological semimetals (TSM) are defined as systems where the conduction and the valence bands cross each other in the Brillouin zone (BZ)

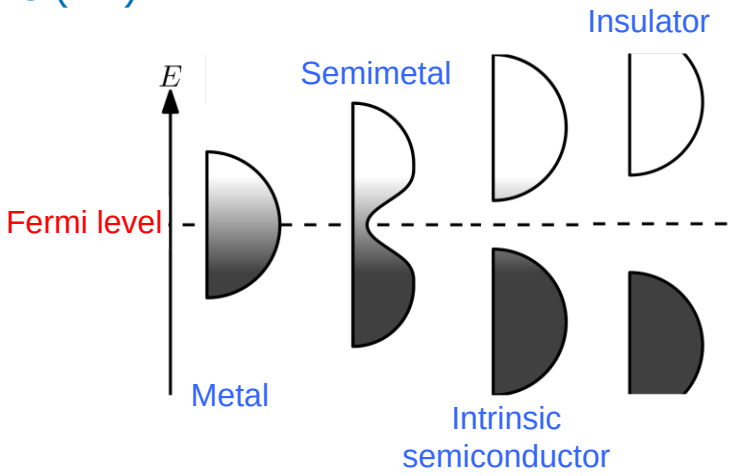

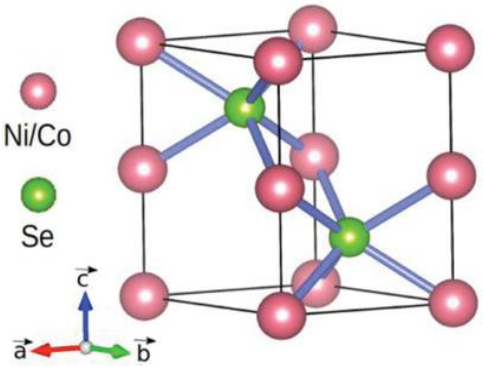

- Hexagonal closed packing (hcp) structure
- Nearly flat bands around ≈1.0 eV below the Fermi level with corresponding peaks in the density of states (DOS) that increase the probability of optical transitions
- The two bands near the Fermi level (in red) give rise to multiple Dirac nodal-line structures

S. Abramovich, [...] E. Curcio, M. Sadan, A. Politano. NiSe and CoSe Topological Nodal-Line Semimetals: A Sustainable Platform for Efficient Thermoplasmonics and Solar-Driven Photothermal Membrane Distillation. Small 18/31 (2022) 2201473

Dielectric function

Occurrence of plasmonic resonance (negative real part)

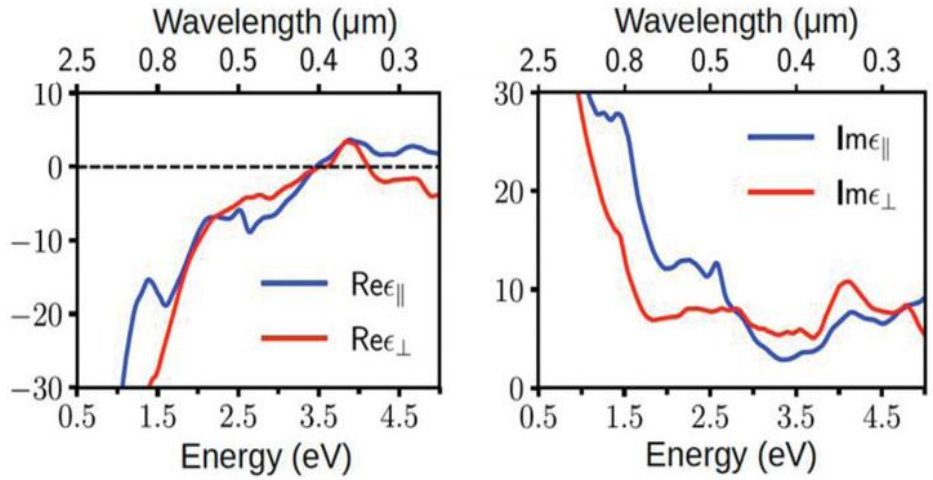

Optimization of NPs size in order to reduce scattering of incoming photons and increasing absorbance (diameter range: 20-50 nm)

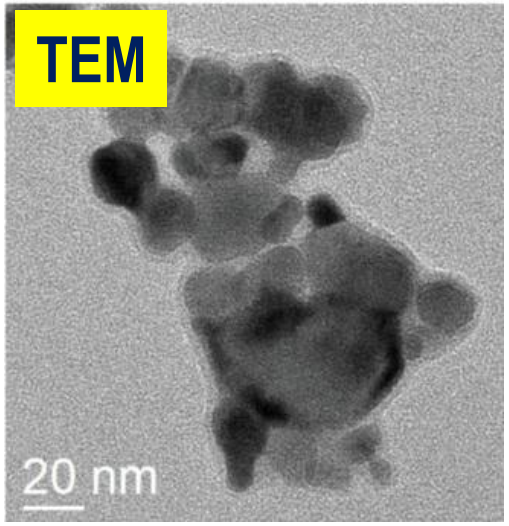

Ag NPs

CoSe NPs

NiSe NPs

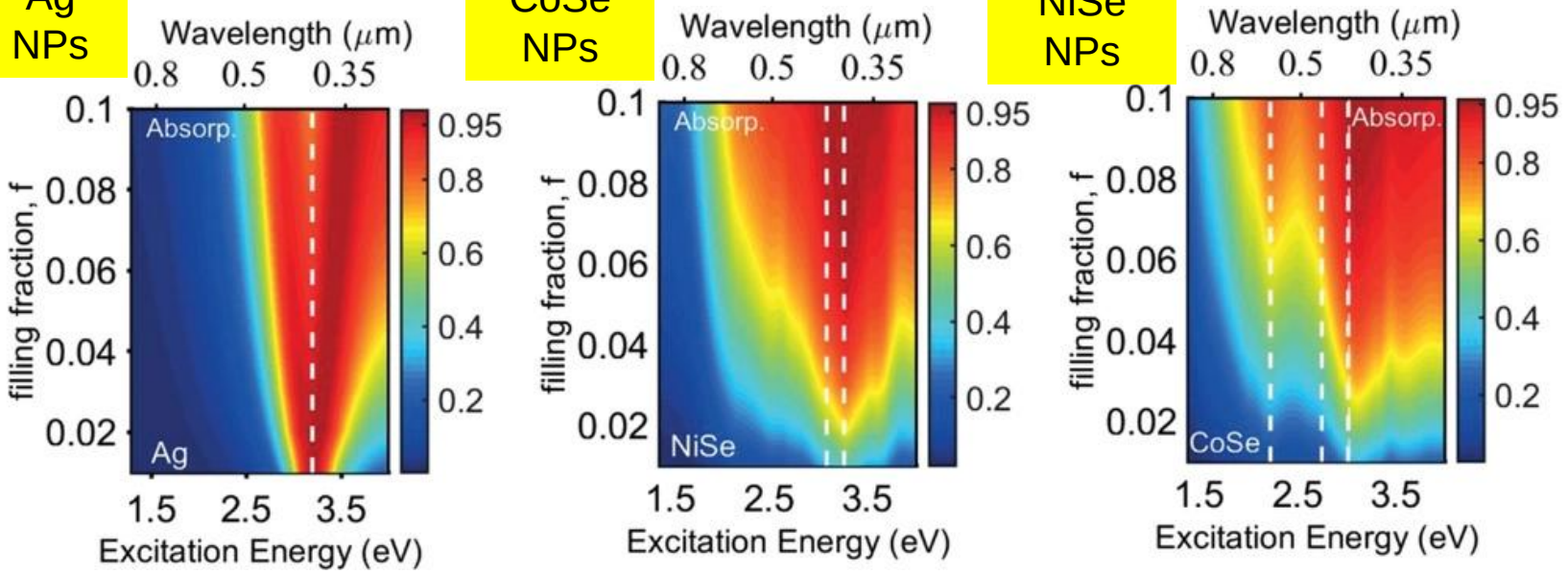

The anisotropic dielectric properties of NiSe and CoSe NPs support multiple localized surface plasmons in the optical range, resulting in a broadband matching with sunlight radiation spectrum

Preparation of composite membranes based on NiSe and CoSe

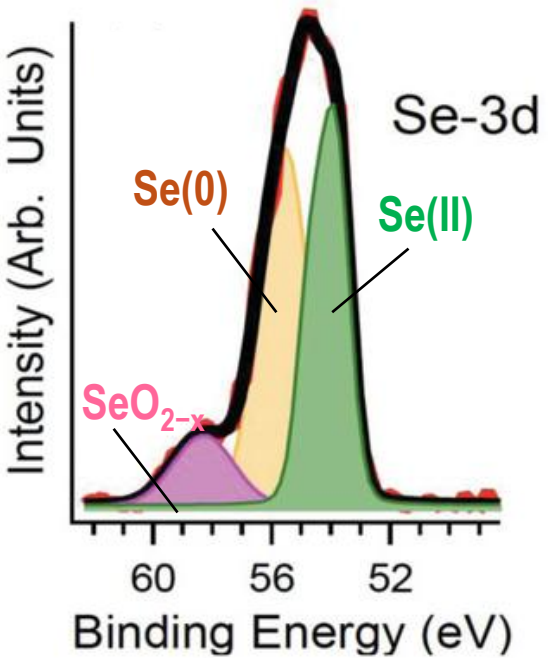

Oxidation is limited (SeO_{2-x} is only the 11% of the spectral area)

Spray Coating

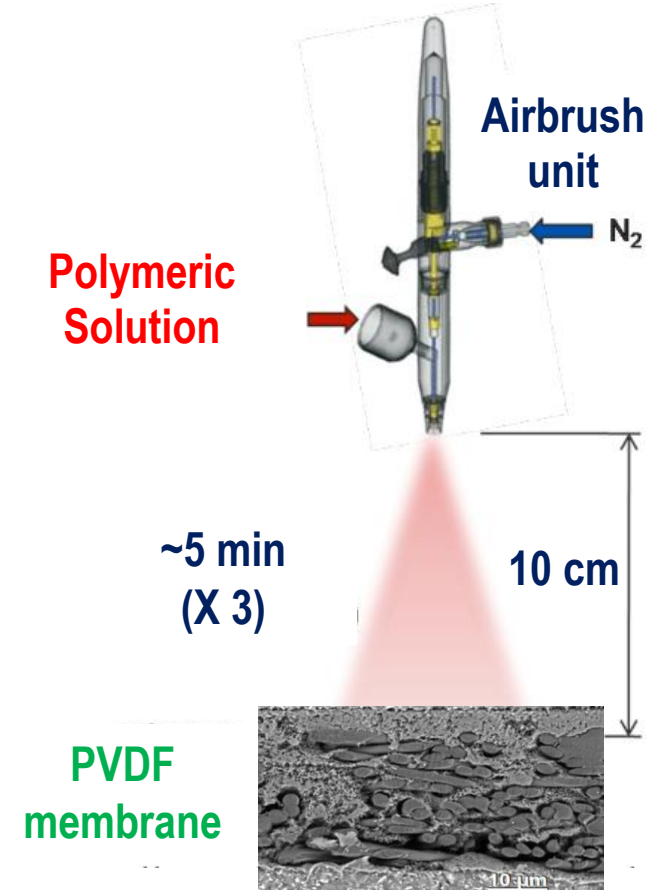

1-sun irradiance (1000 W/m²)

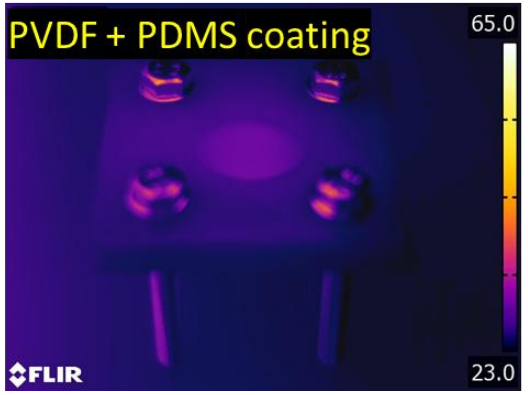

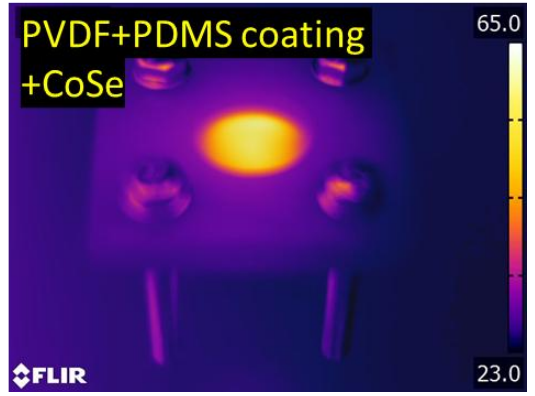

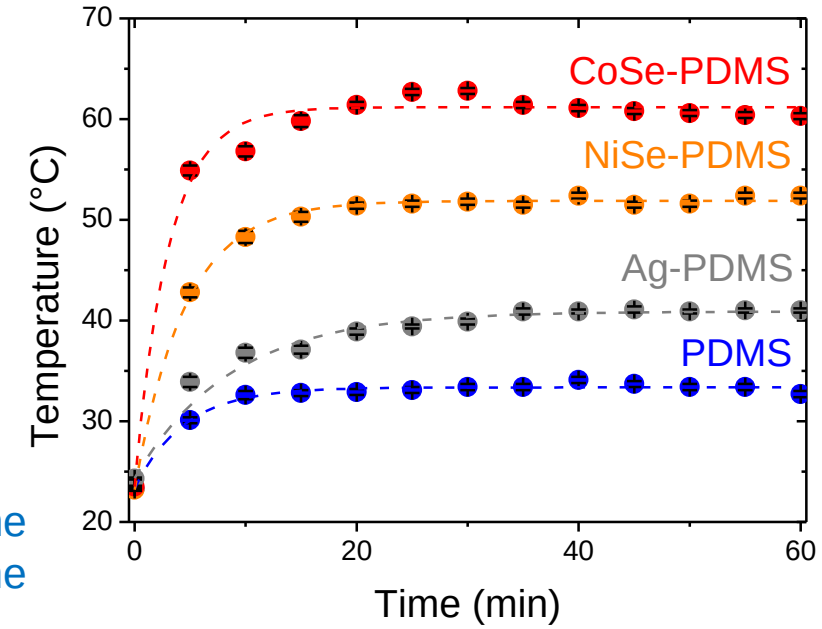

PVDF support coated with a thin porous polydimethylsiloxane $(C_2H_6OSi)_n$ (PDMS) layer embedding NiSe or CoSe NPs: increases the transmembrane flux by 330% and 690%, respectively.

Photothermal Materials for efficient PhMD

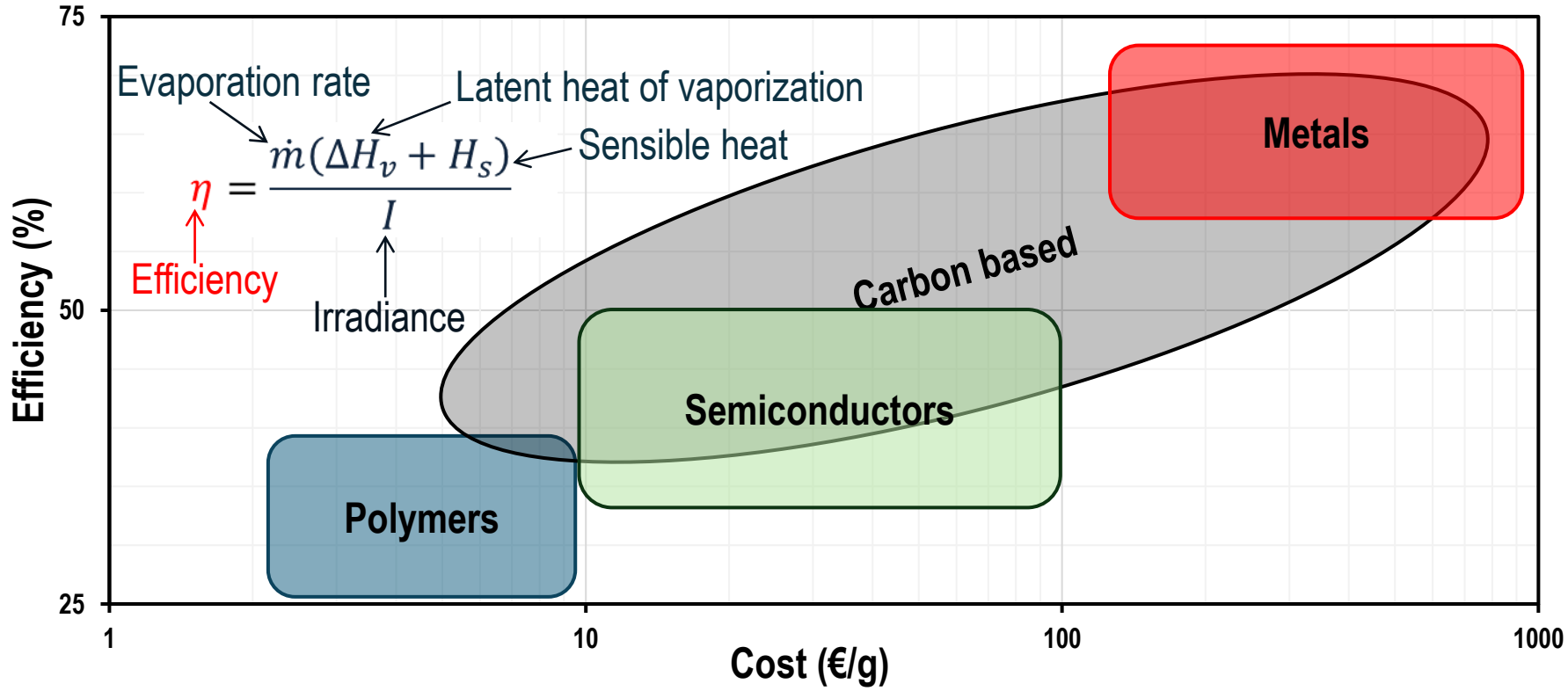

- Composite membranes to reduce the cost of the membrane and localize the light-to-heat conversion on membrane surface
- Development of photothermal membranes able to exploit the solar radiation

Dimensionally controlled graphene-based surfaces for Photothermal Membrane Distillation-Crystallization

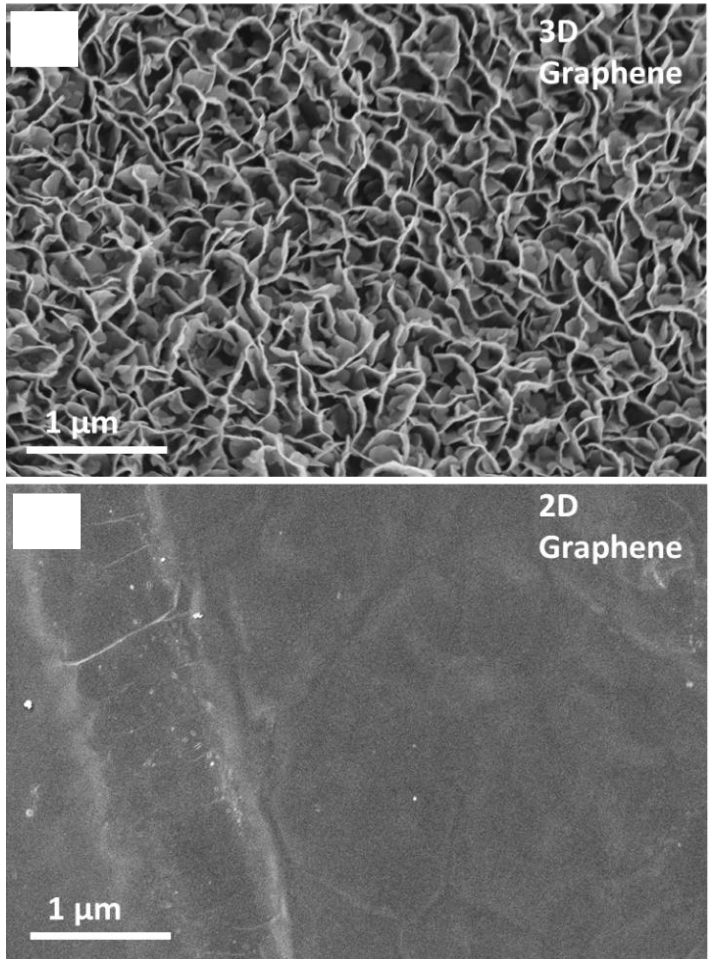

- ❑ Three dimensional vertically orientated graphene sheet arrays (3D-G)
- ❑ Two-dimensional graphene thin films (2D-G)

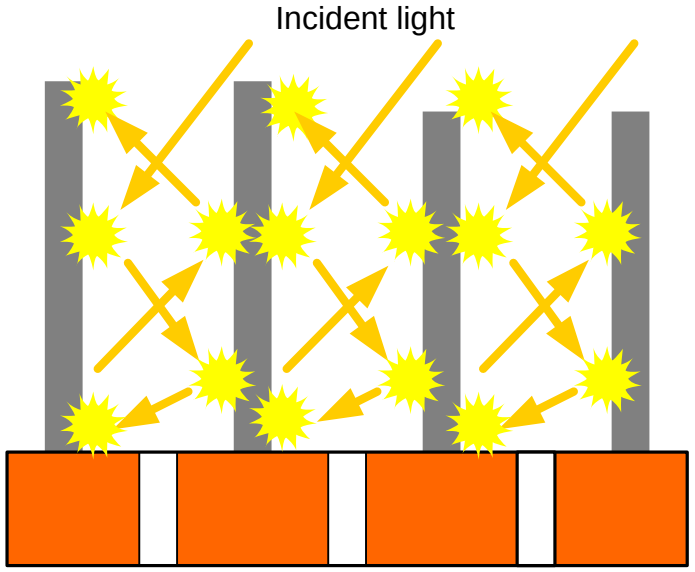

3D-G interconnected graphene flakes promoting light trapping effects

Near-100% light absorption across the entire UV–Vis-NIR

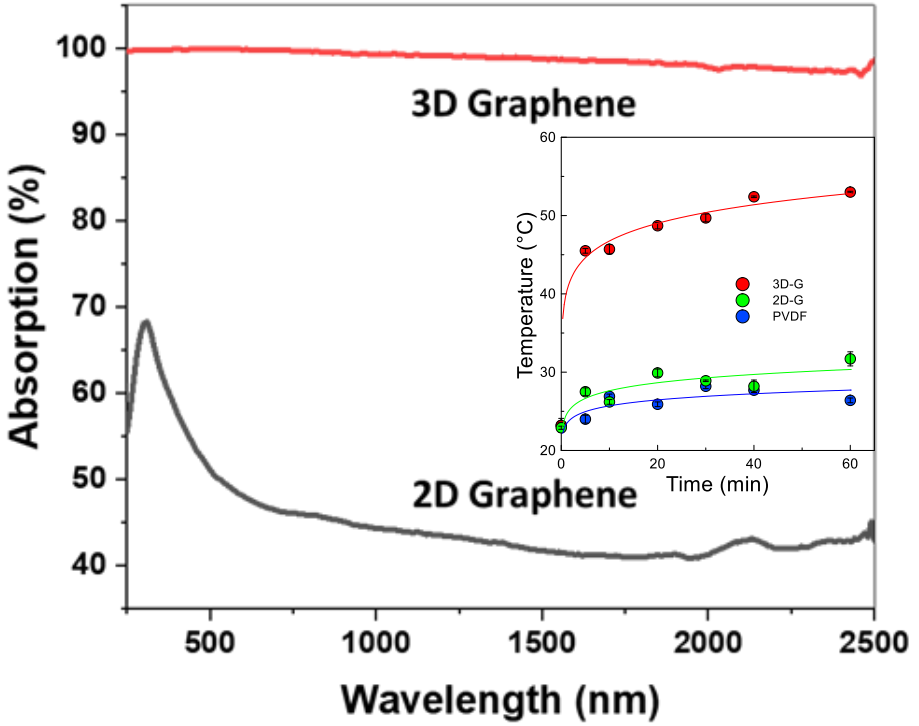

S. Santoro, M. Aquino, D. H. Seo, T. van Der Laan, M. Lee, J. S. Yun, M. J. Park, A. Bendavid, H. K. Shon, A. H. Avci, E. Curcio. Dimensionally controlled graphene-based surfaces for photothermal membrane crystallization. Journal of Colloid and Interface Science 623 (2022) 607

FROM MEMBRANE DISTILLATION TO MEMBRANE CRYSTALLIZATION

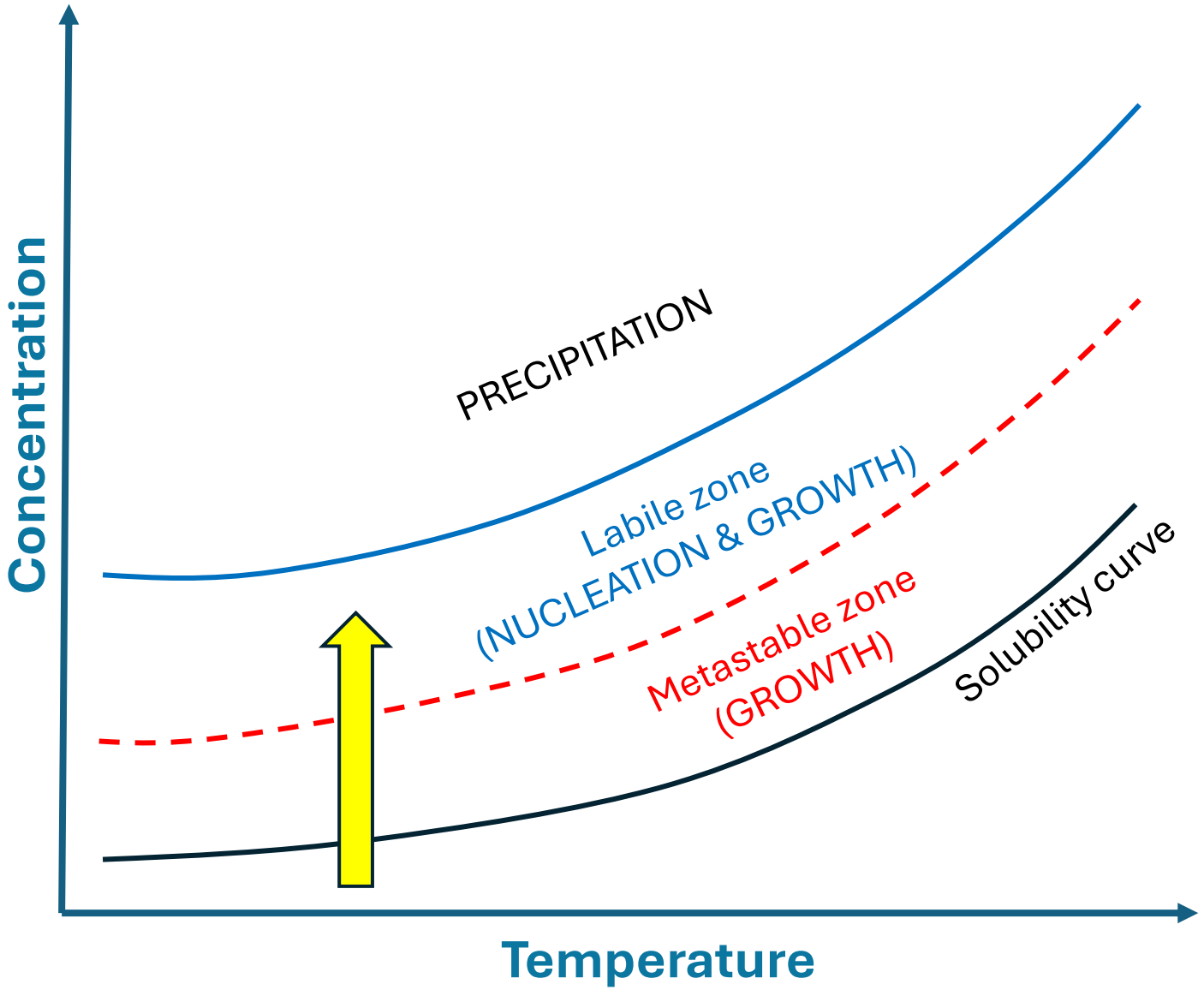

The solution is progressively concentrated up to supersaturation by evaporating the solvent through microporous hydrophobic membranes.

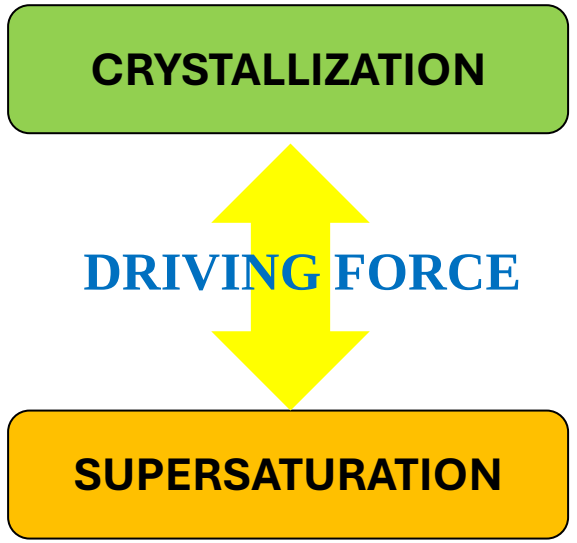

$$S = \frac{c}{c^*}$$

MEMBRANE CRYSTALLIZATION OF INORGANIC SALTS

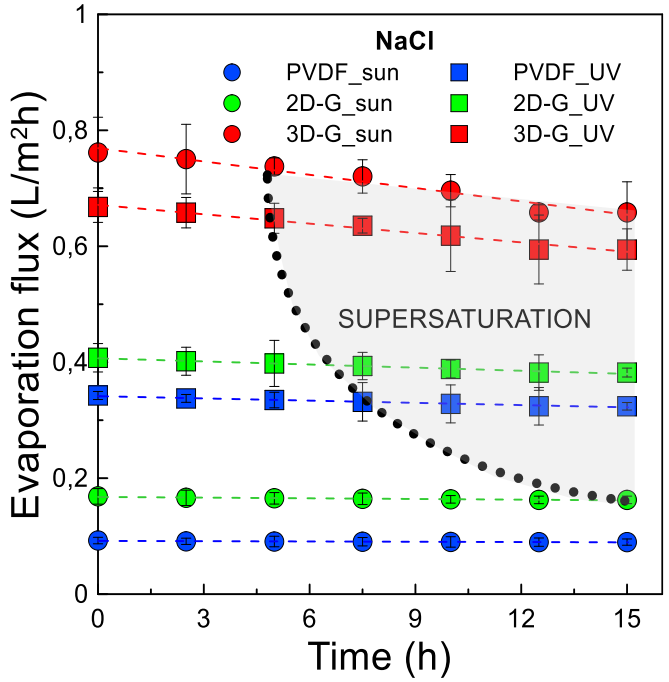

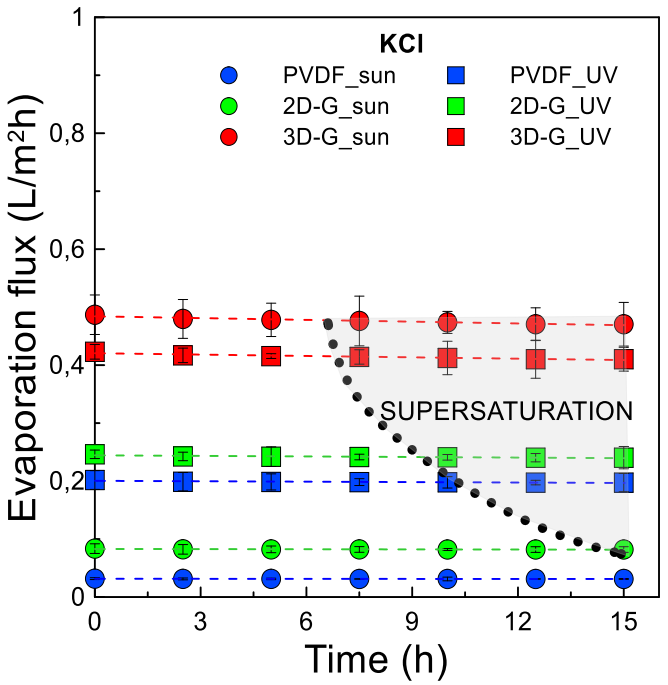

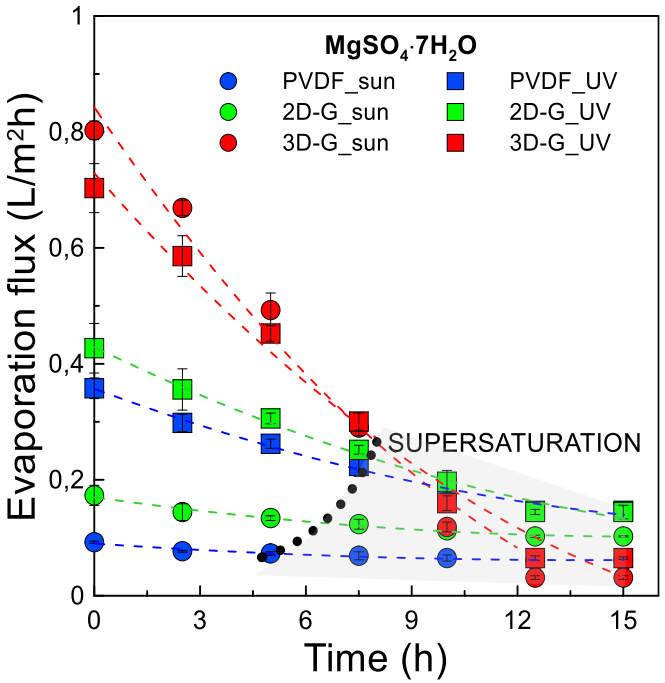

Solubility 20→60°C

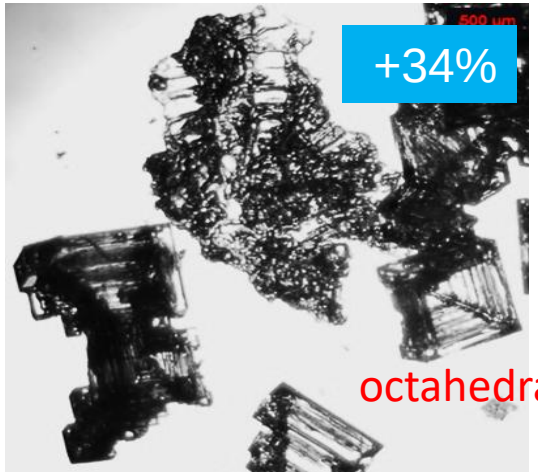

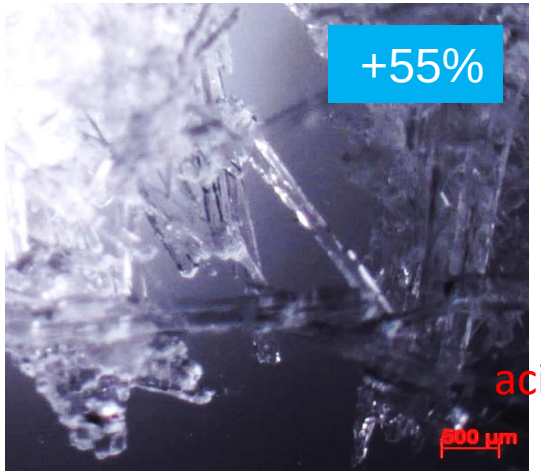

High supersaturation

Low supersaturation

SOLAR EVAPORATION PONDS

Salt Lakes

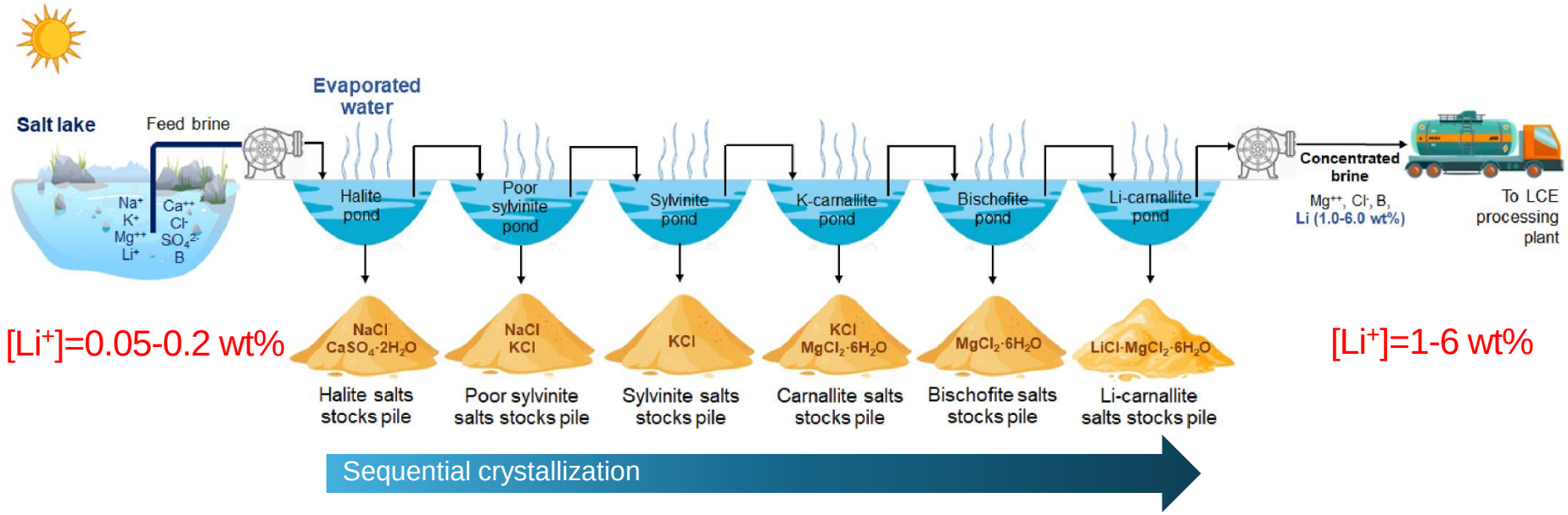

- Evaporated water: **18,000 – 60,000 m^3 day^{-1} (>1,000 m^3 ton^{-1} of Li)**
- **Evaporation rate <0.3 kg m^{-2} h^{-1}**
- **High residence time (12-24 months, depending on local weather conditions) which determines high requirement of pond volume and area**
- **85-95% of total water lost**

Adapted from : Cerda, A., Quilaqueo, M., Barros, L., Seriche, G., Gim-Krumm, M., Santoro, S., Avci, A.H., Romero, J., Curcio, E., Estay, H., 2021. Recovering water from lithium-rich brines by a fractionation process based on membrane distillation-crystallization. J. Water Proc. Eng. 41, 102063

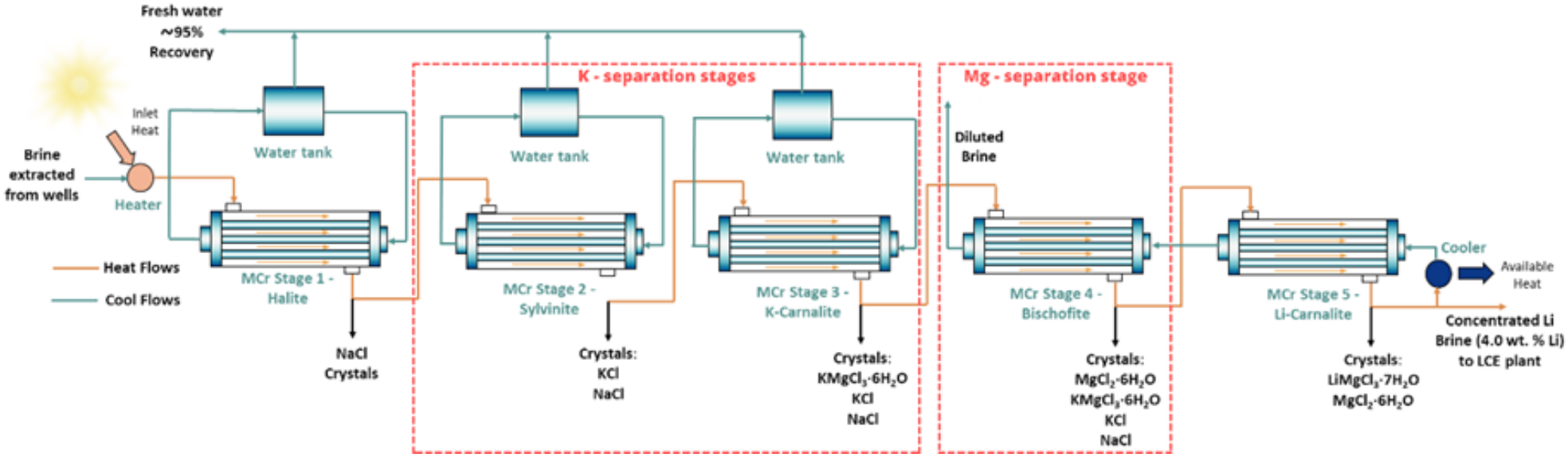

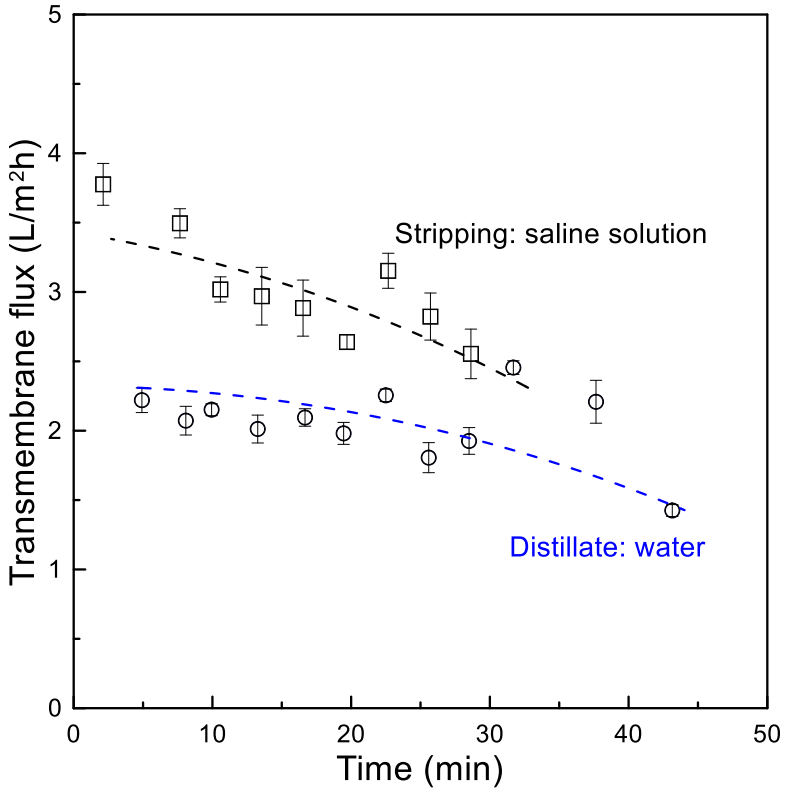

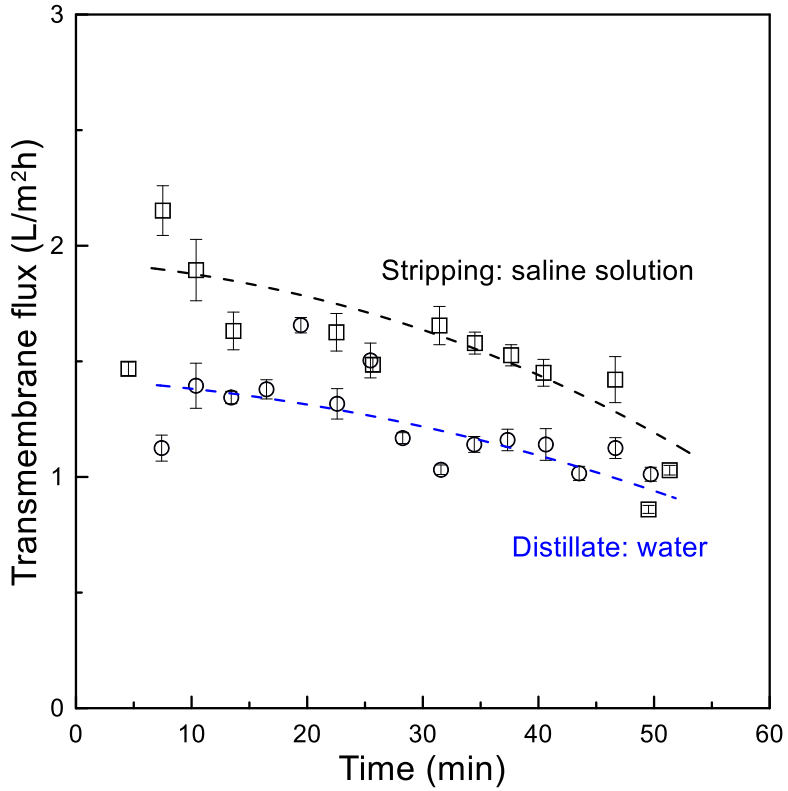

M. Quilaqueo, […], S. Santoro, E.Curcio, H. Estay. Membrane distillation-crystallization applied to a multi-ion hypersaline lithium brine for water recovery and crystallization of potassium and magnesium salts. Desalination 586 (2024) 117895

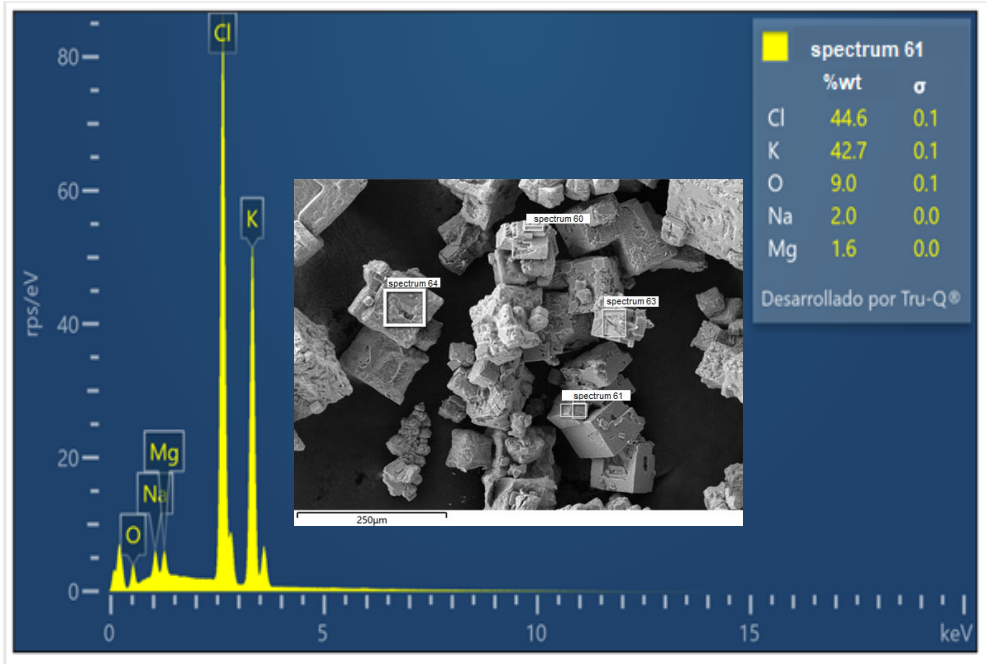

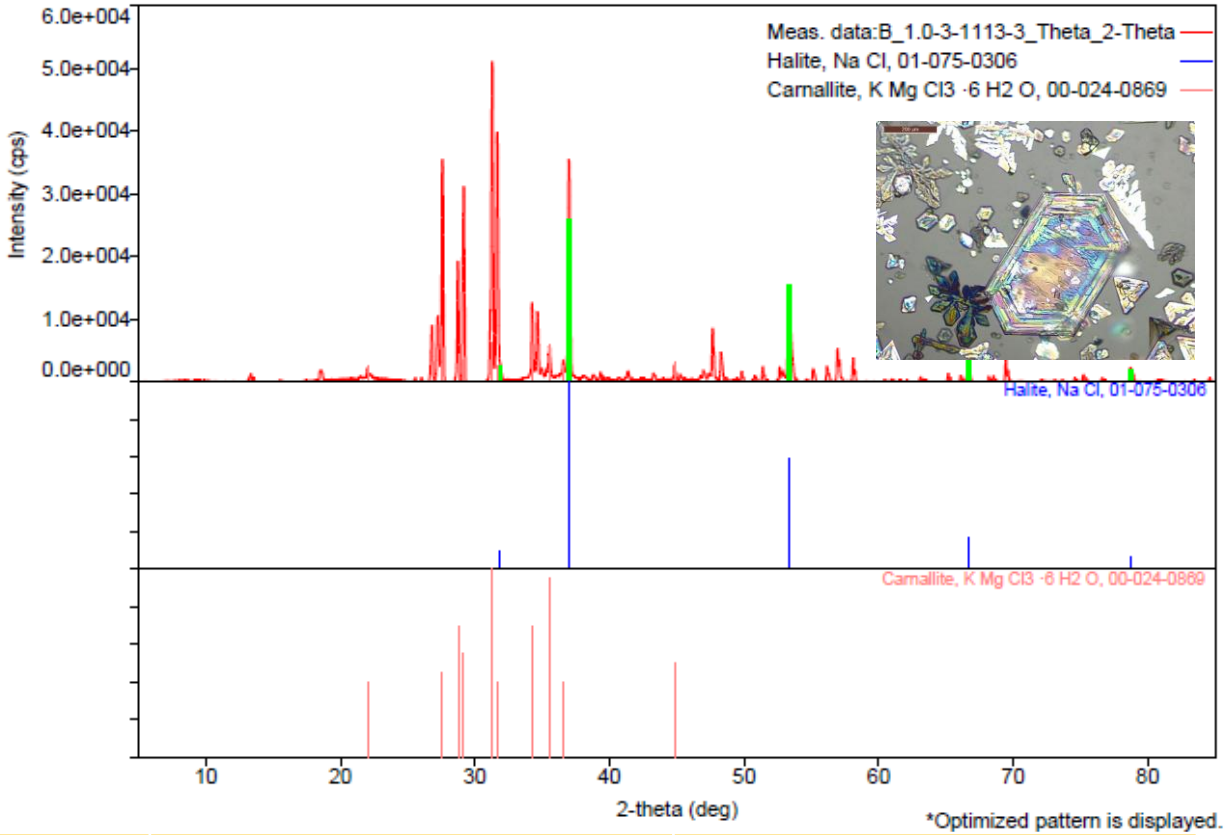

Water recovery %	%wt Na in the crystallized salt	%wt K in the crystallized salt	%wt Mg in the crystallized salt
83%	38.1	1.7	-
93%	35.3	3.9	0.72

M. Quilaqueo, G. Seriche, C. González, G. Piaggio, L, Barros, F. Gallardo, S. Díaz-Quezada, D. Zamora, B. Barraza, R. Ruby-Figueroa, S. Santoro, E. Curcio, H. Estay. Membrane distillation-crystallization applied to a multi-ion hypersaline lithium brine for water recovery and crystallization of potassium and magnesium salts. Desalination 586 (2024) 117895

Photothermally-assisted Evaporator/Crystallizer

the CENTURIUM PRIZE جائزة القرن
RETHINK BRINE challenge

MAGNE TO

ReThink Brine Proposal
Round 3

launched by Sandooq Al Watan - UAE

Associated Organizations

جامعة خليفة
Khalifa University

UNIVERSITÀ DELLA CALABRIA

هيئة البيئة - أبوظبي
Environment Agency - ABU DHABI

EWEC

صندوق الوطن
SANDOOQ AL WATAN

ALDAR

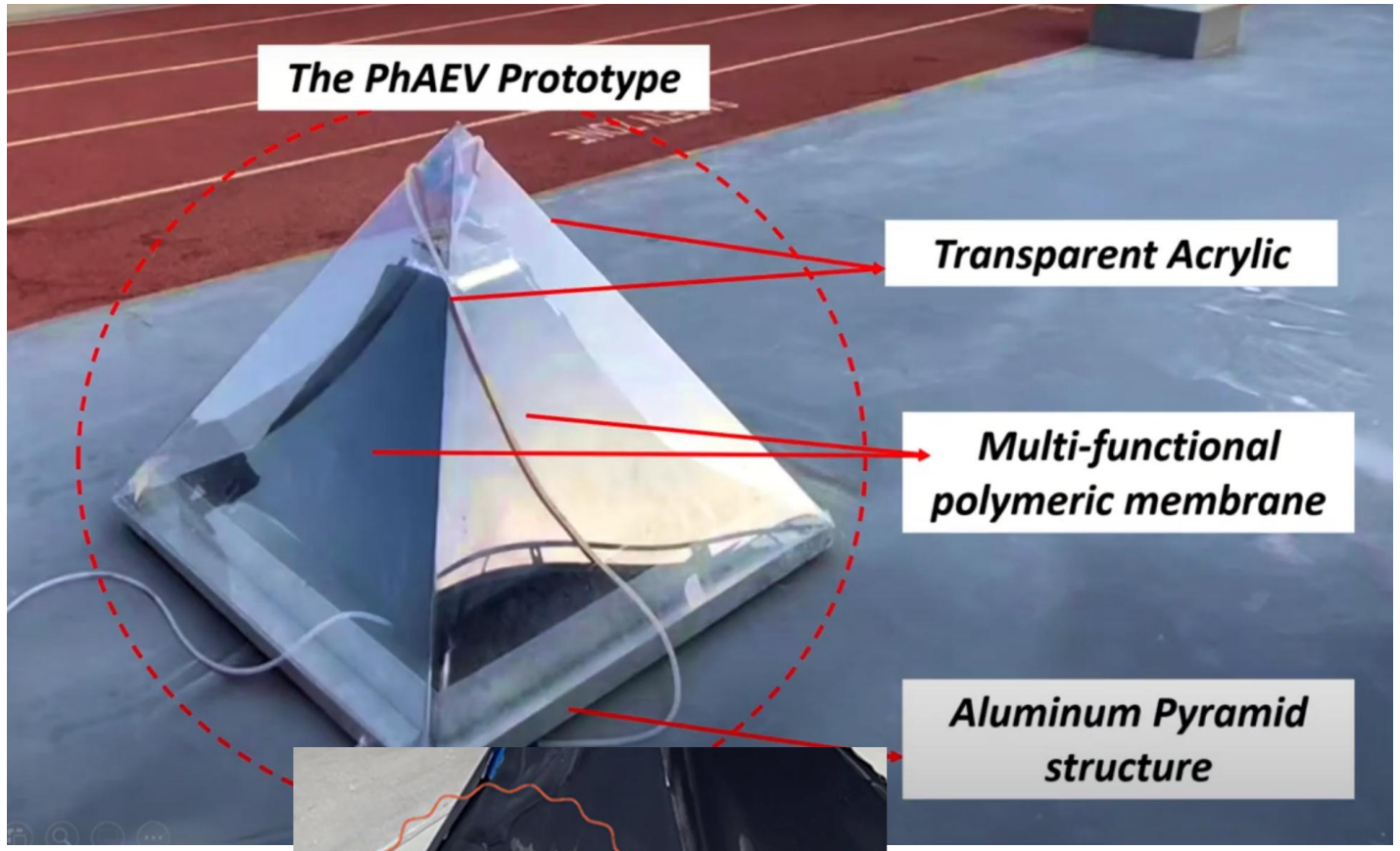

- Concentrate seawater desalination brine - halite crystallization
- Recovery Magnesium
- Possible extension to sequential crystallization

https://www.youtube.com/watch?v=eEo180HQCKo

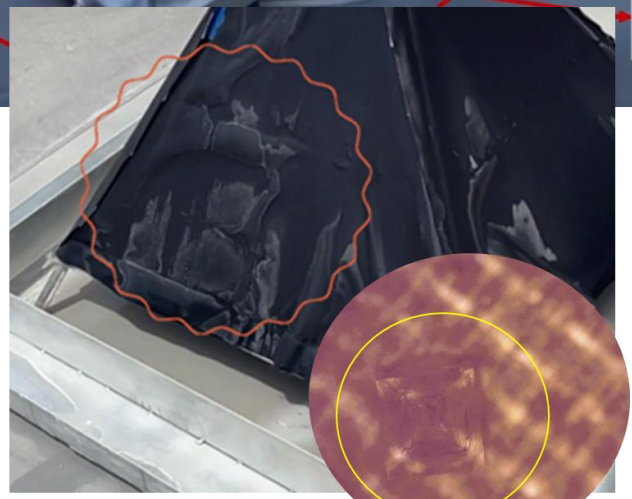

NaCl nucleation

Tungsten Disulfide (WS_2) nanosheets for LiCl Membrane Crystallization

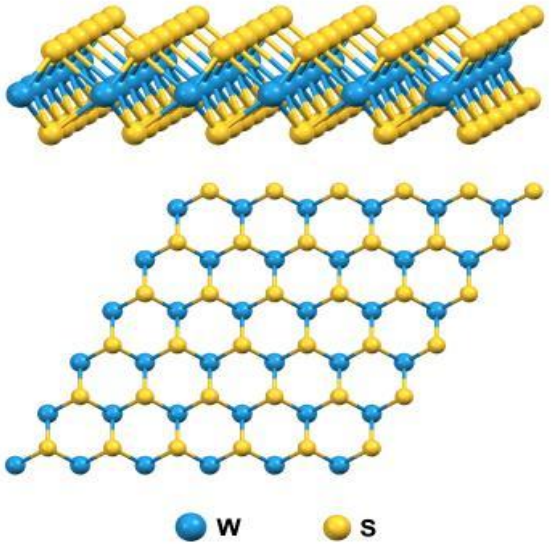

Conduction band

Valence band

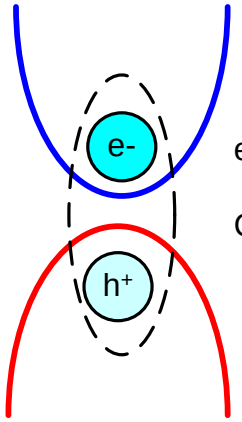

electron and a electron hole are attracted to each other by the Coulomb force to form a bound state called an exciton

WS_2 displays a high-permittivity excitonic resonances in the visible region

Transition metal dichalcogenides are van der Waals semiconductors (multiple 2D layers of transition metal atoms sandwiched between two layers of chalcogen atoms)

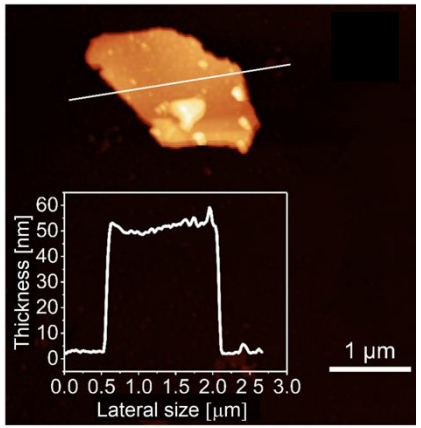

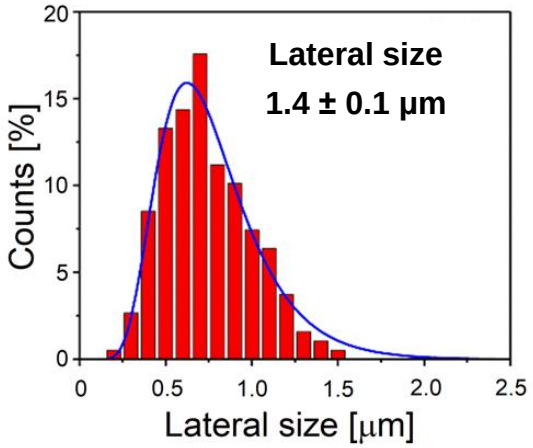

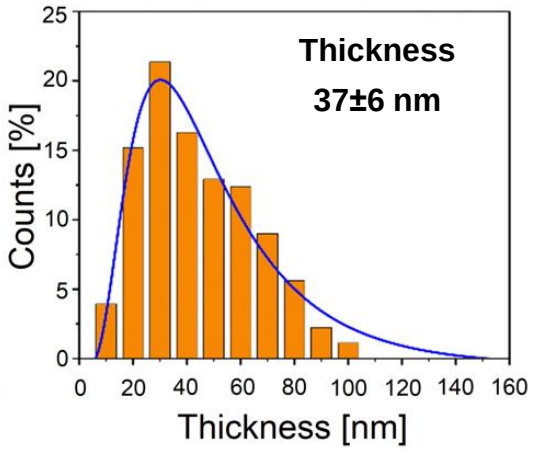

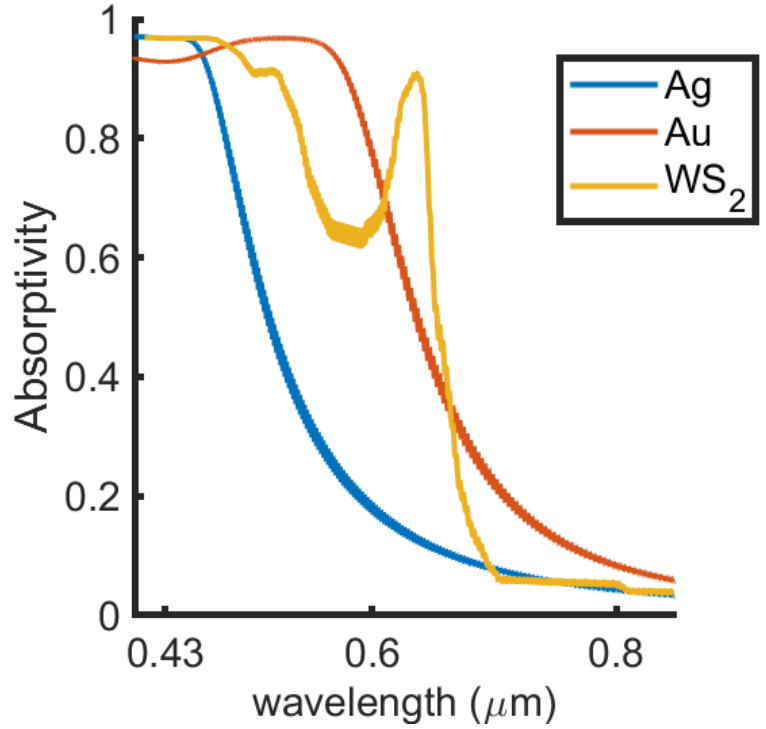

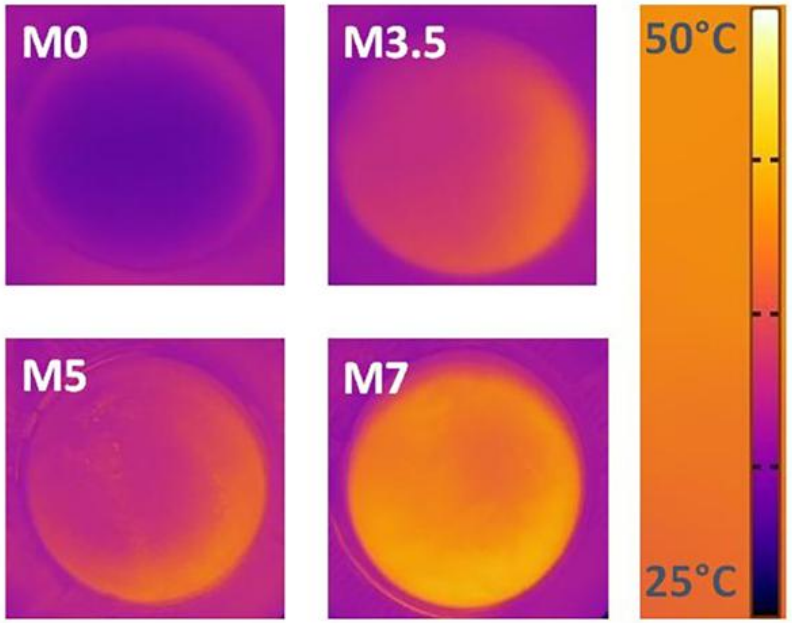

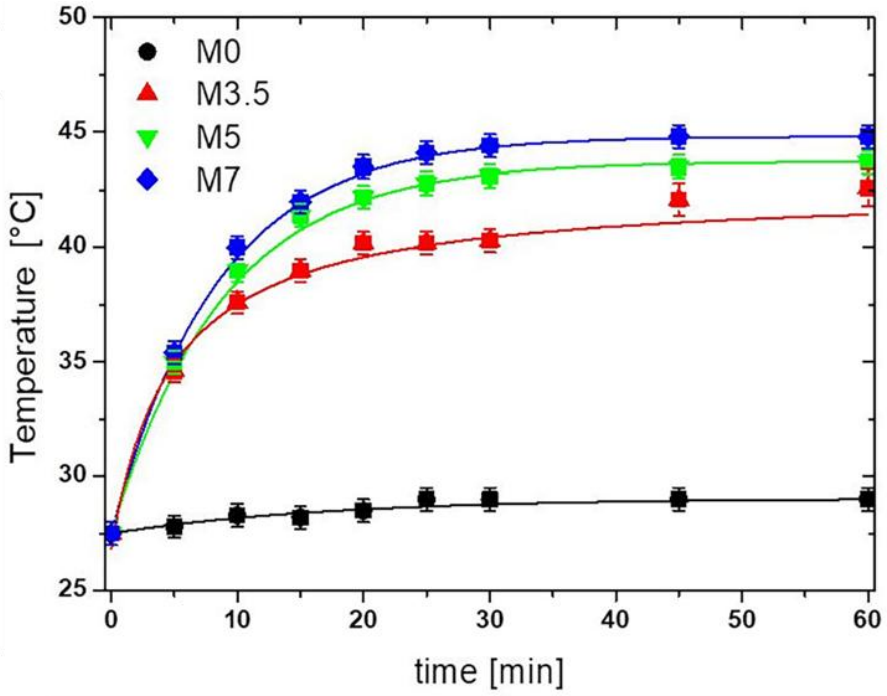

The maximum heating rate observed under sunlight irradiation is 1.44 K·min^{-1} at the highest nanofiller loading (M7), corresponding to a maximum temperature increase of ca. 15 °C.

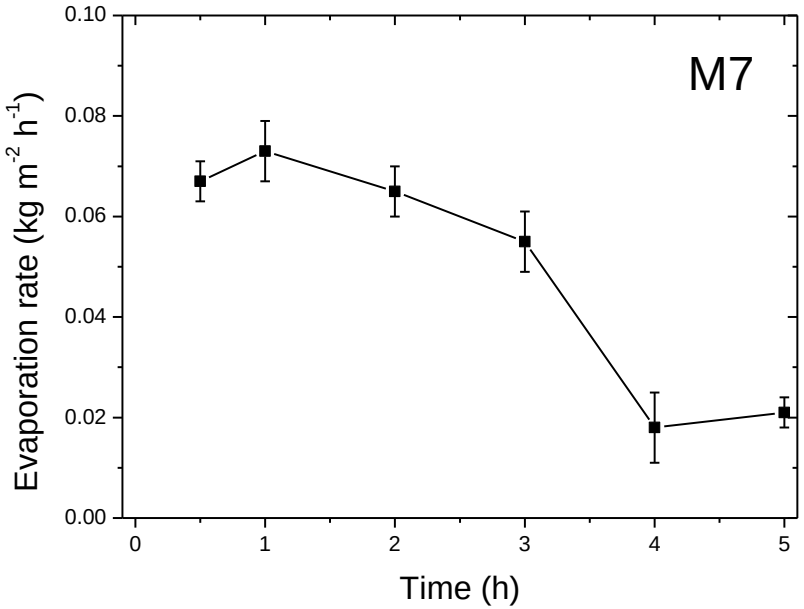

LiCl crystals, needle-like morphology, aspect ratio 10:1, average size: 150 ± 60 µm

HETEROGENEOUS NUCLEATION ON POROUS MEMBRANES

Gibbs free energy of the crystalline phase

$$\Delta G = \Delta G_{vol} + \Delta G_{surf} = -\frac{\Delta\mu}{\Omega}V + \gamma A_L - (\gamma_s - \gamma_i)A_{SL}$$

Energy gained upon formation of a bulk phase

Energy required to form a new surface

CLASSICAL NUCLEATION THEORY (CNT)

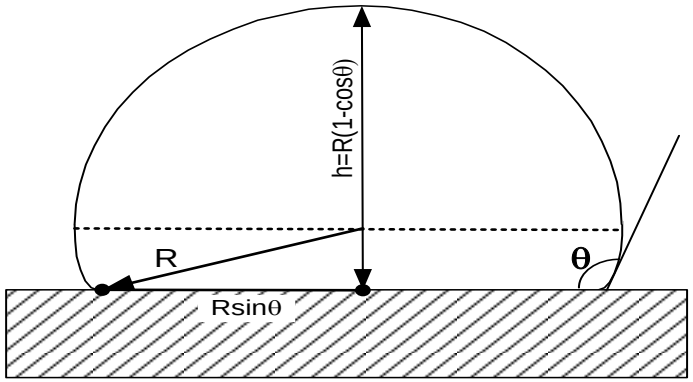

Young' equation

for ideal flat surfaces

$$(\gamma_S - \gamma_i) = \gamma_L \cos\theta$$

$$\frac{\Delta G^*_{het}}{\Delta G^*_{\hom}} = \frac{1}{4}(2+\cos\theta)(1-\cos\theta)^2$$

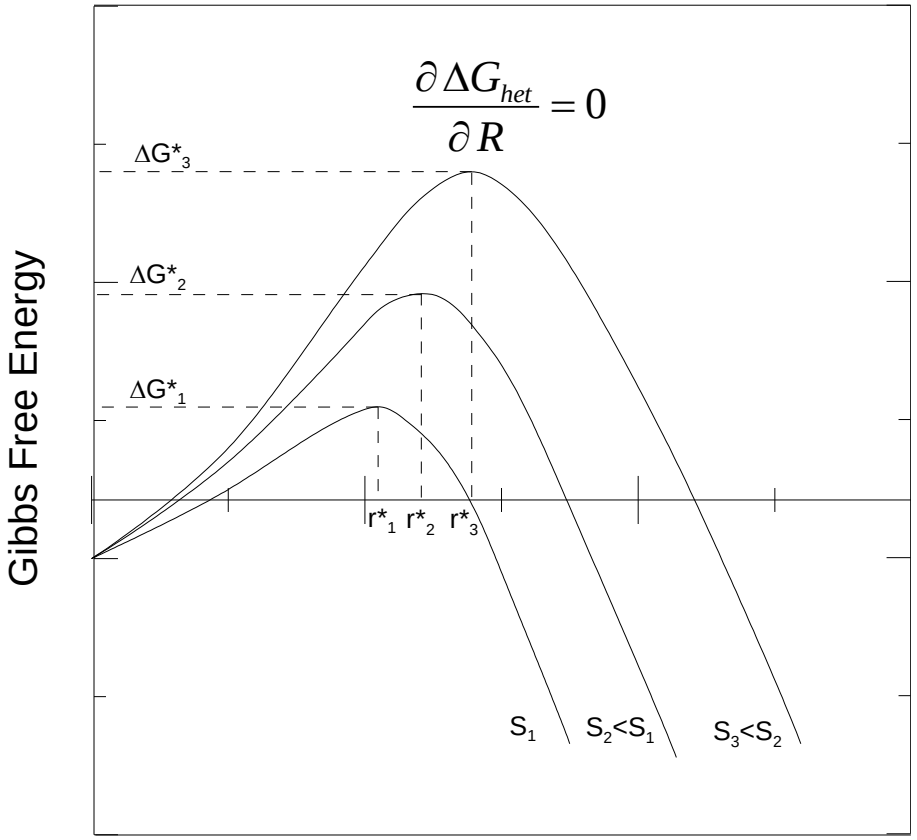

The formation of a crystalline nucleous is an **activated process**. It can occur if an energy barrier is overcome.

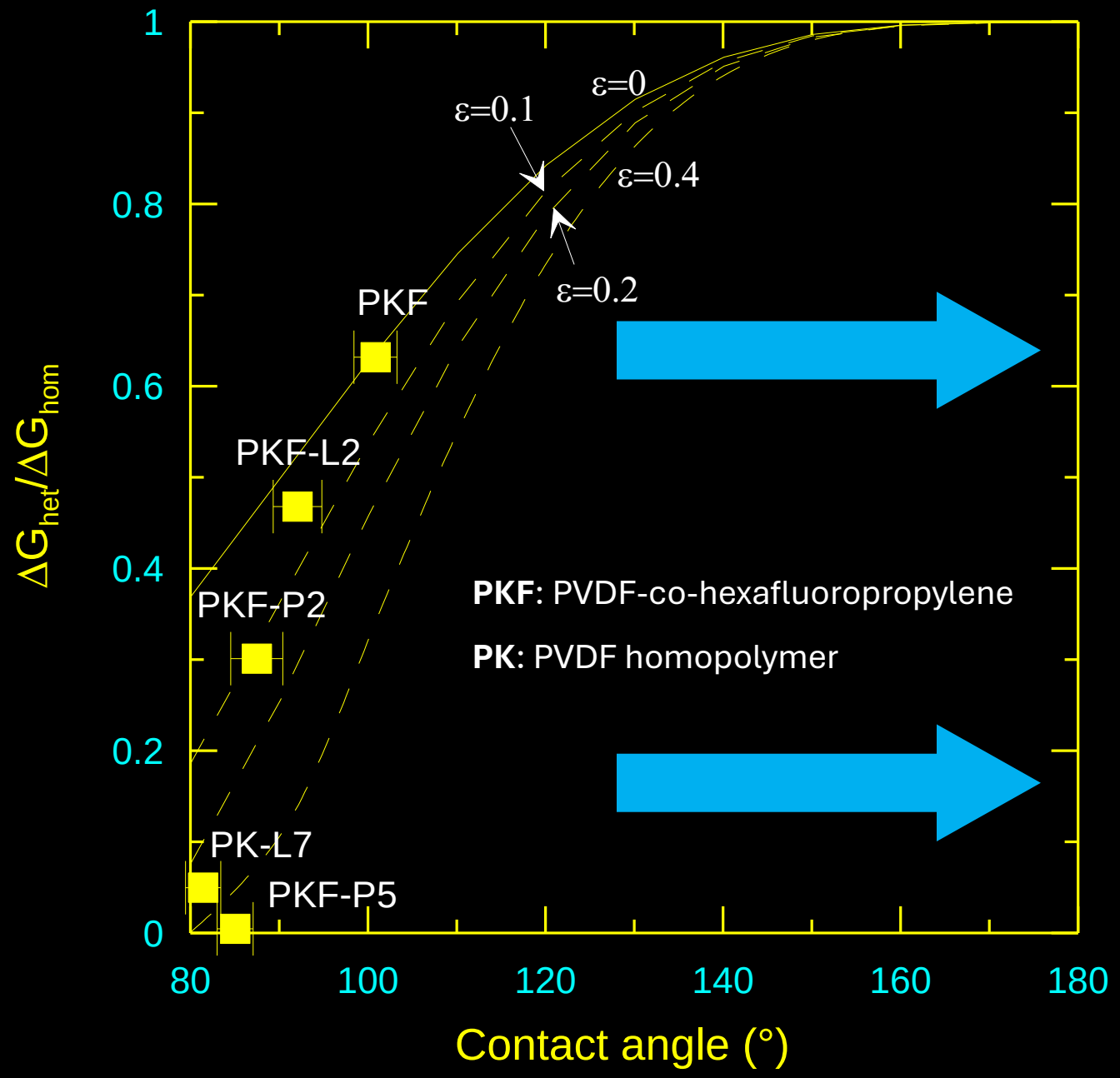

↑porosity ↔ ↓ΔG

↑contact angle ↔ ↑ΔG

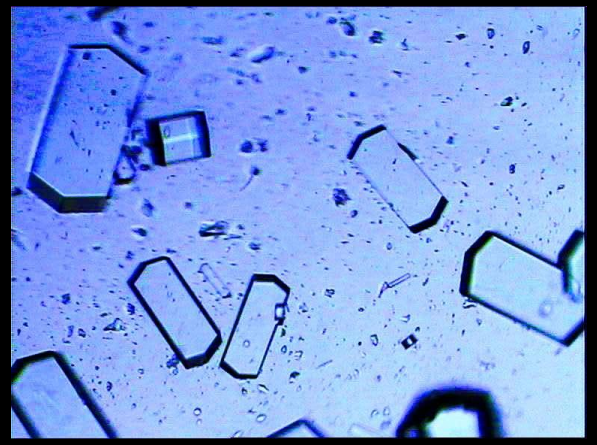

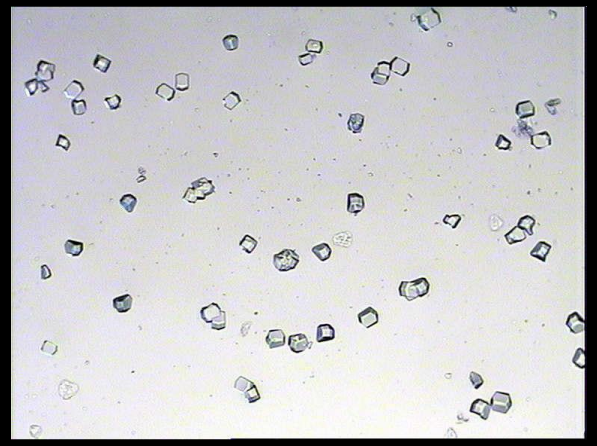

Lysozyme crystals

THE WAY TOWARDS SUPERSATURATION

Temperature difference

$$\Delta p = p_w^0\left(T_{feed}^m\right) \cdot x_{w,feed} \cdot \gamma_{w,feed} - p_w^0\left(T_{dist}^m\right)$$

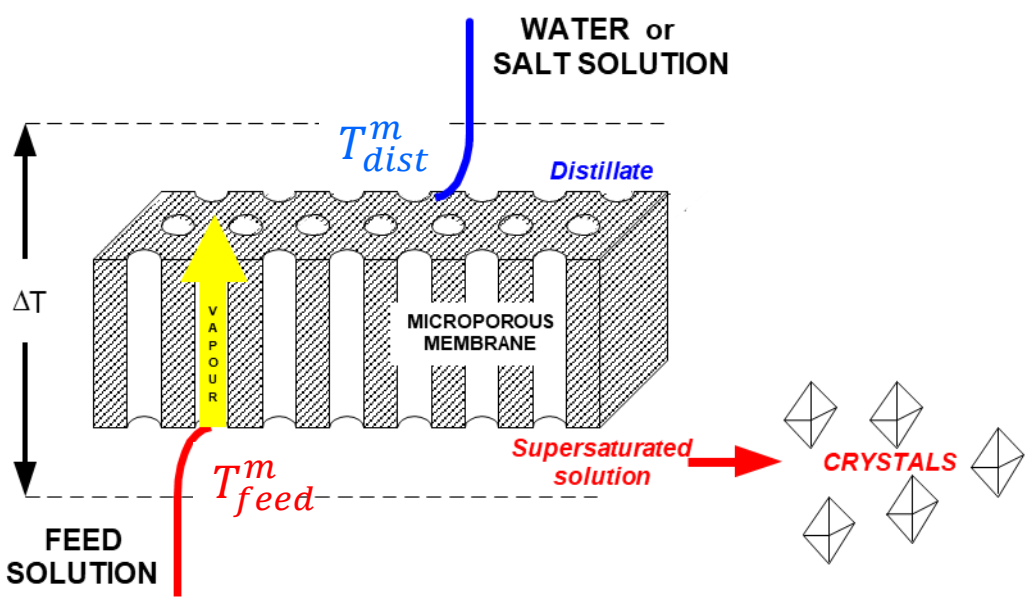

Concentration difference

$$\Delta p = p_w^0\left(T_{feed}^m\right) \cdot x_{w,feed} \cdot \gamma_{w,feed} - p_w^0\left(T_{strip}^m\right) \cdot x_{w,strip} \cdot \gamma_{w,strip}$$

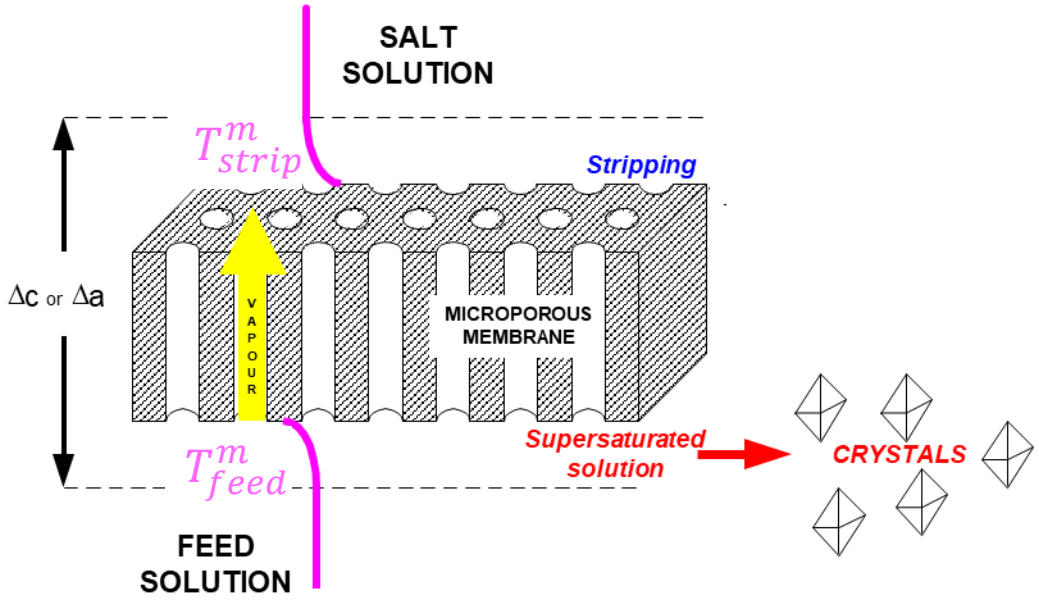

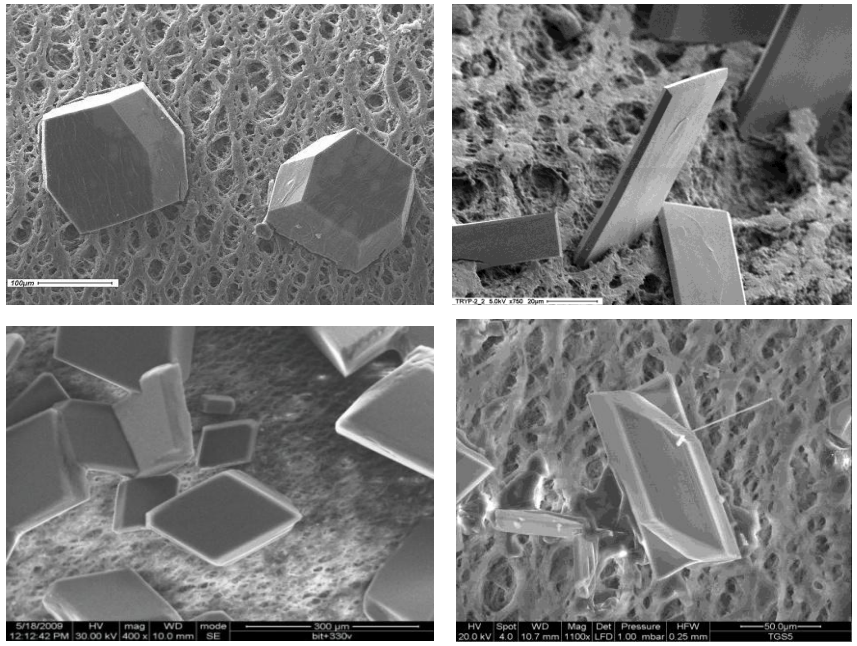

NUCLEATION RATE

$$J(t) \propto \exp\left(-\frac{t}{\tau}\right)$$

INDUCTION TIME

INDUCTION TIME (Time elapsed between the achievement of supersaturation and the appearance of first crystals): shortened by using membrane with respect to conventional crystallization techniques

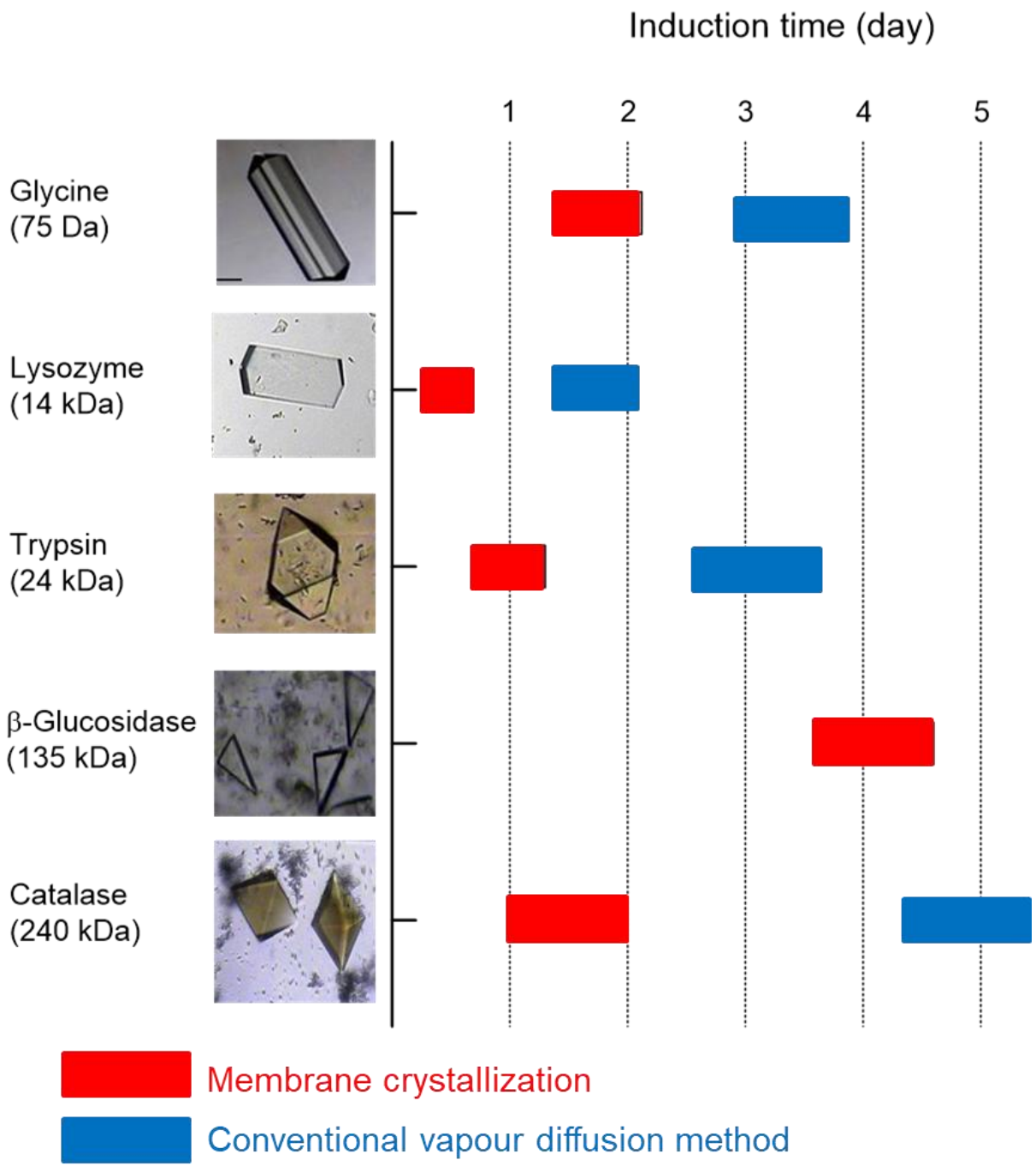

FAST BUT ORDERLY: LYSOZYME

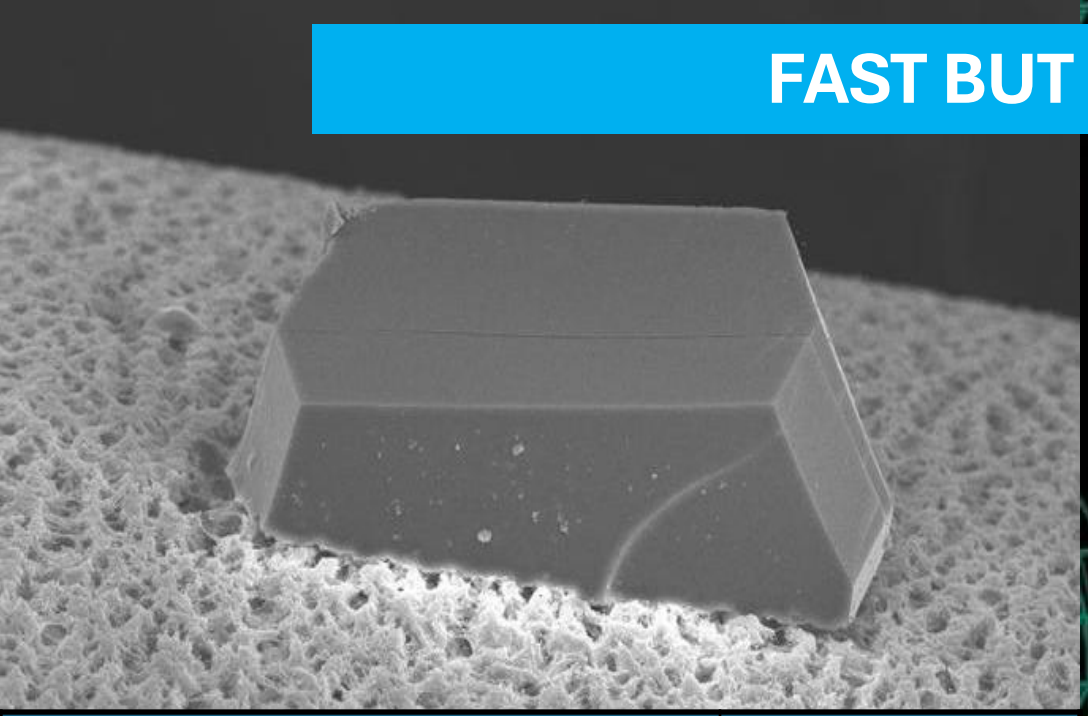

		HEWL
Dimensions	Linear (mm)	0.25 x 0.20 x 0.11
	Volume (mm^3)	5.5×10^{-3}
Space Group	$P\,4_3\,2_1\,2$	
Cell	a (Å)	79.403
	b (Å)	79.403
	c (Å)	37.832
Mosaicity (°)		0.167
Resolution	Overall (Å)	15.6 - 1.91
	Last Shell (Å)	1.93 - 1.91
$\langle I/\sigma(I) \rangle$	Overall	37.0
	Last Shell	16.3
B_{Wilson} ($Å^2$)		20.4

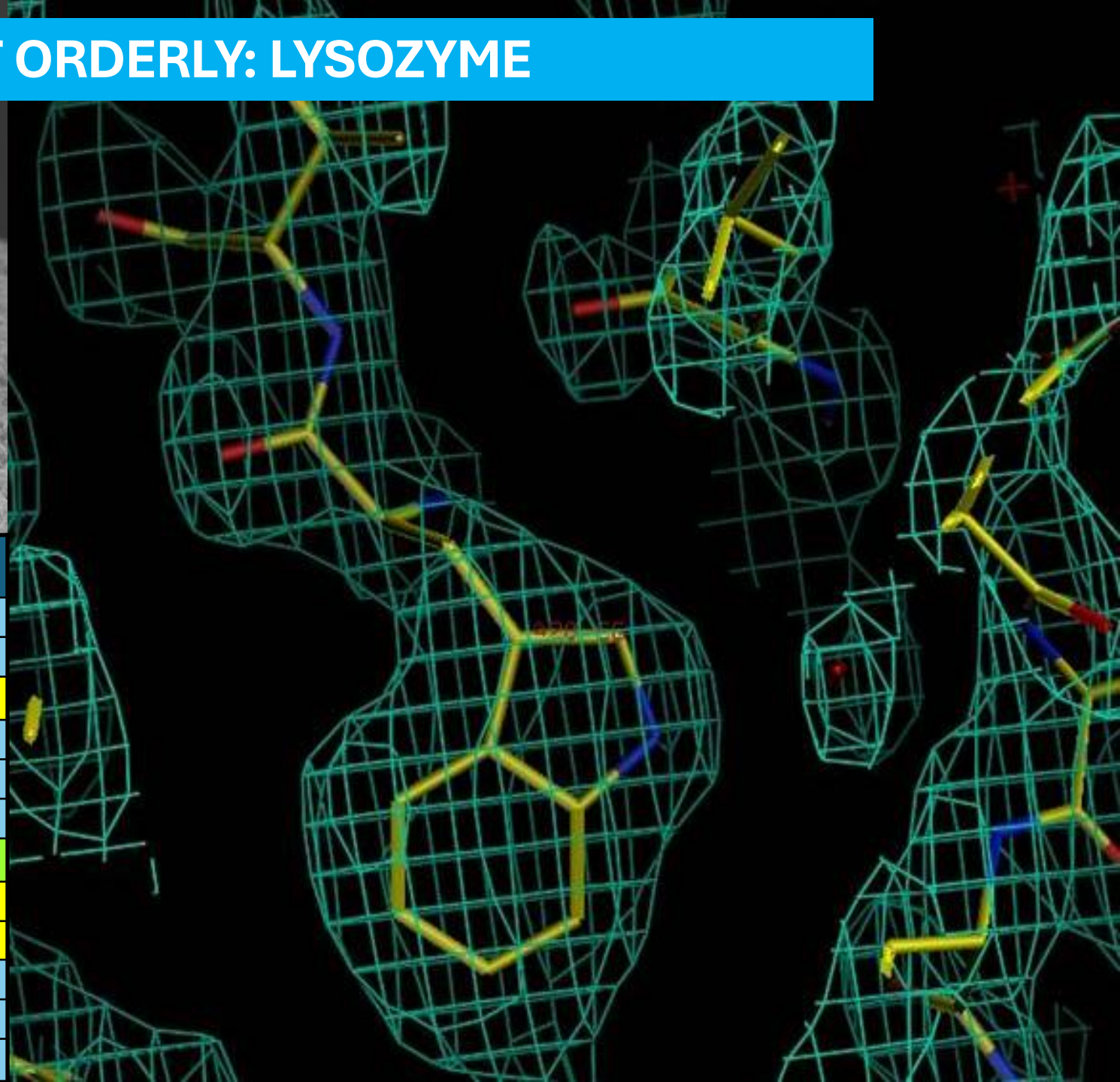

POLYMORPHISM SELECTION

In crystallography, **polymorphism** is the phenomenon where a compound or element can crystallize into more than one crystal structure. Polymorphism in drugs can also have direct medical implications since dissolution rates depend on the polymorph.

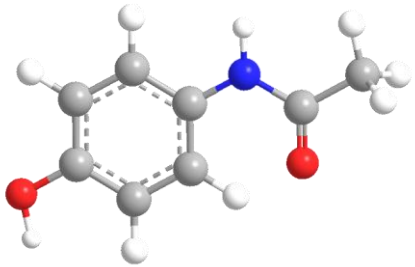

PARACETAMOL

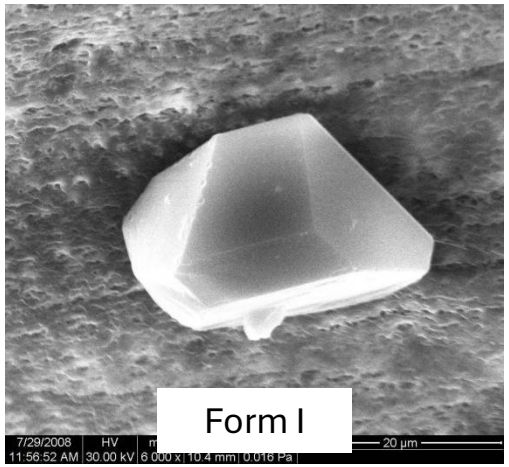

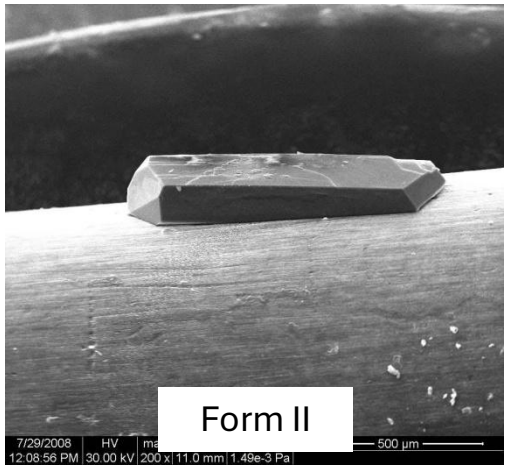

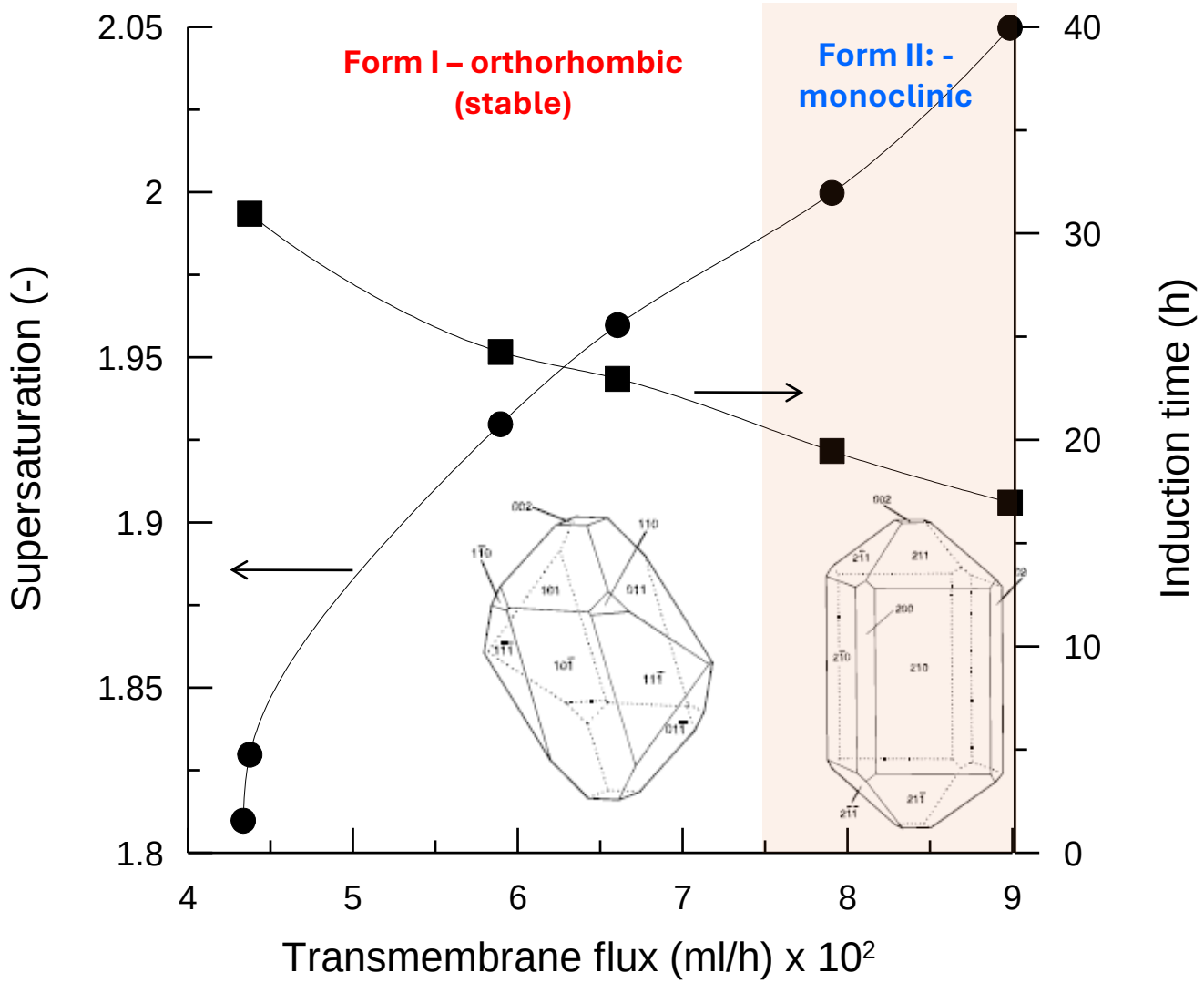

EFFECT OF SURFACE CHEMISTRY: INDUCTION TIME

Nucleation is inherently a stochastic event and an energy-activated process. The aleatory nature of the nucleation stage reflects the variability of induction time measurements, that is the period elapsed from attainment of a given supersaturation until the formation of crystals with critical size

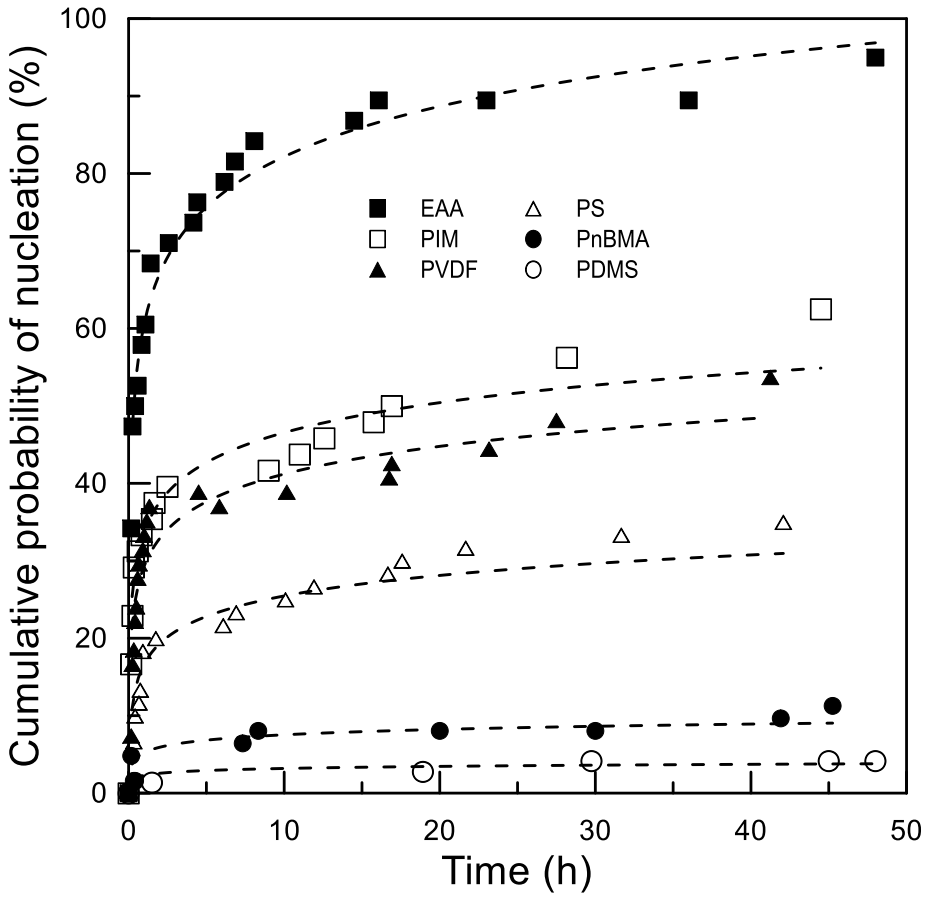

$$P = e^{-t/\tau}$$

Probability of nucleation

Induction time

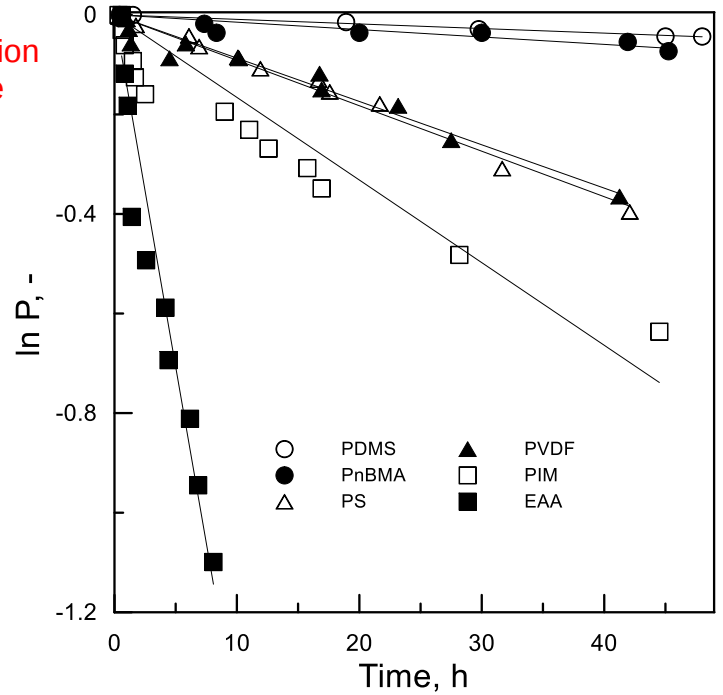

Polymeric surface	Average induction time (τ, h)	Contact angle (θ ,°)
Polydimethylsiloxane	1310	95.9±1.6
Poly-n butyl methacrylate	478	81.4±1.2
Polystyrene	117	80.3±2.3
Polyvinylidene fluoride	101	73.9±1.1
Polyimide	67.6	56.6±2.4
Ethylene/Acrylic acid (15%) cop.	11.5	99.8±4.0

Strong H-bonds between Acrylic Acid and paracetamol

Percentage of samples/vials crystallized (tests on 64 vials) on different polymeric surfaces as a function of time. Experimental conditions: 30 g_{ACM}/kg H_2O, 10°C, 800 μL solution

The hydroxyl groups of the ACM molecules aligned along {001} plane appear perpendicularly oriented towards the polymeric surface, thus indicating that EAA copolymer is interacting through hydrogen-bonding.

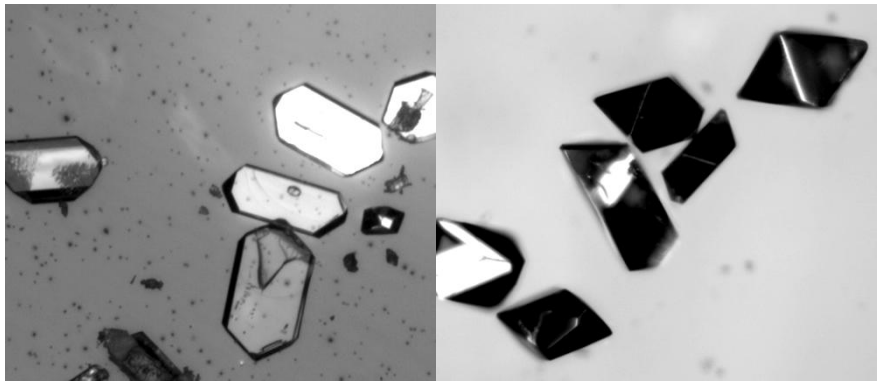

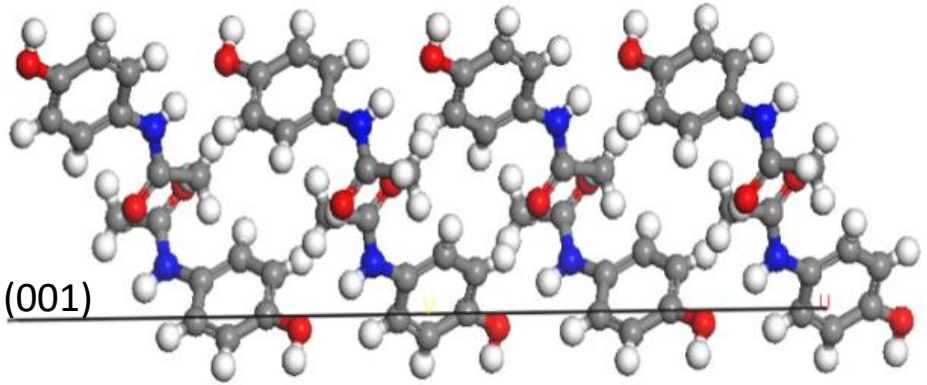

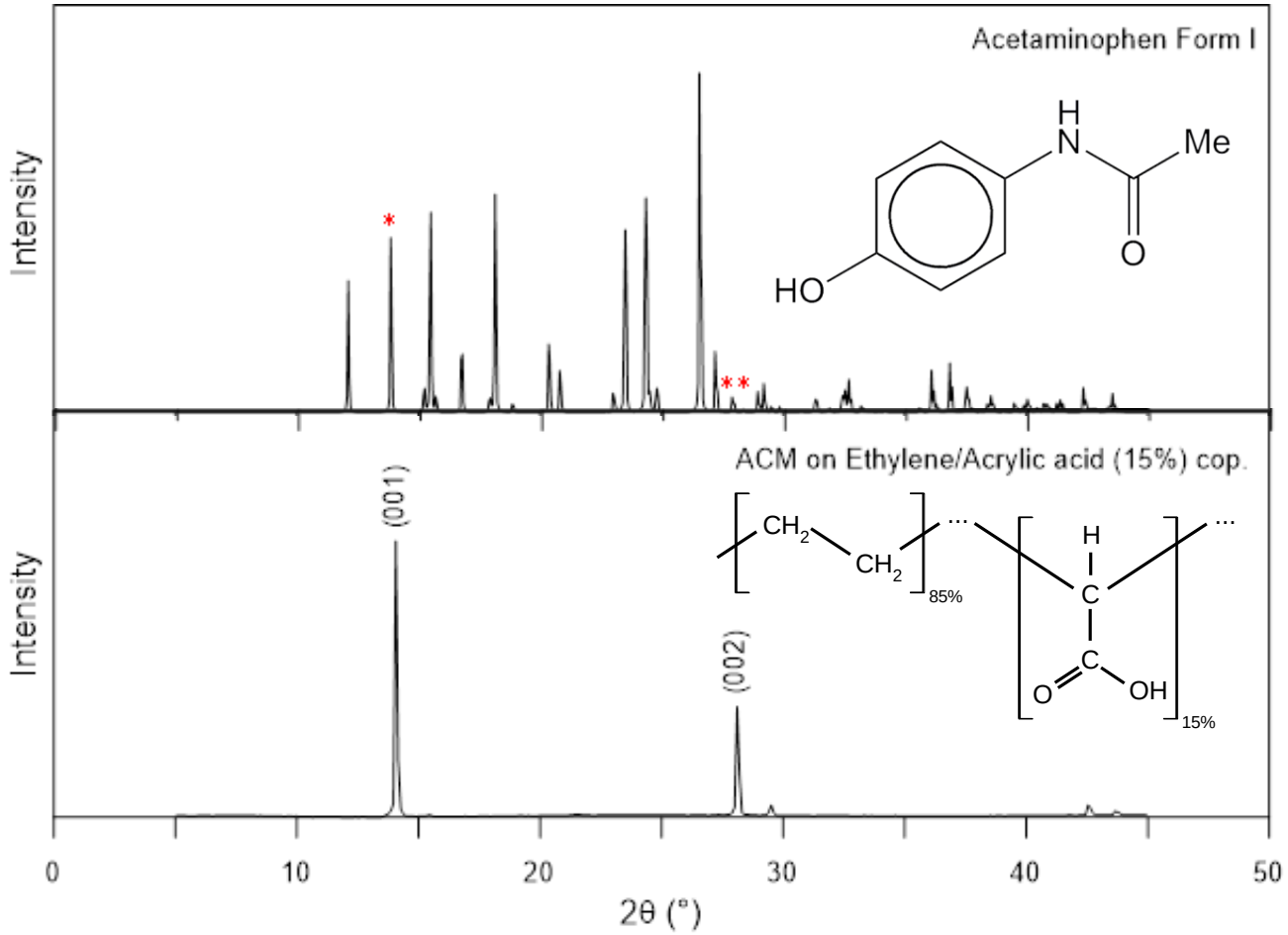

Major reflection at 15.0° is related to the preferential growth of form II crystals along the plane (111) with hydroxyl groups of ACM obliquely oriented towards the substrate. Interfacial interactions are likely to involve both imide functionality and carbonyl groups in polyimide.

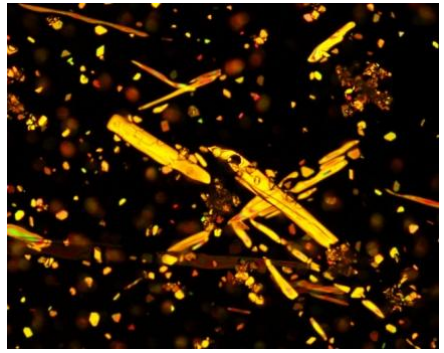

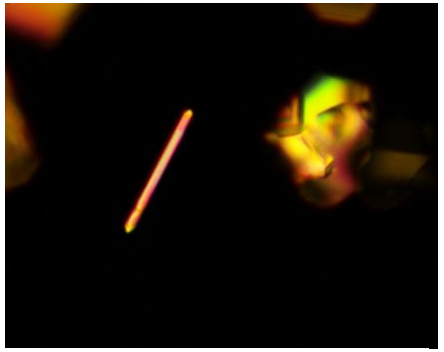

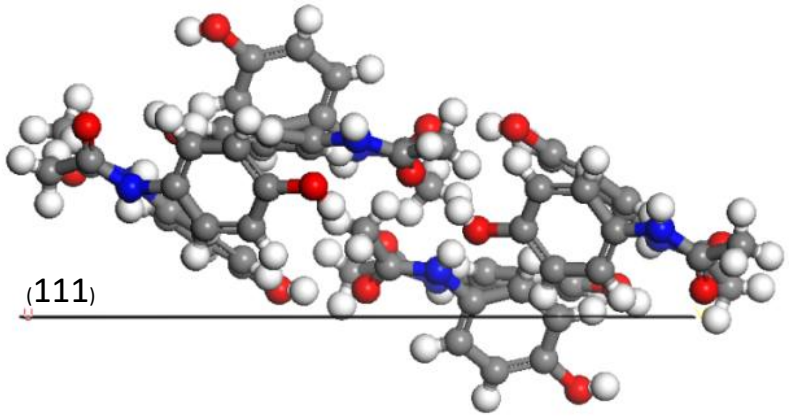

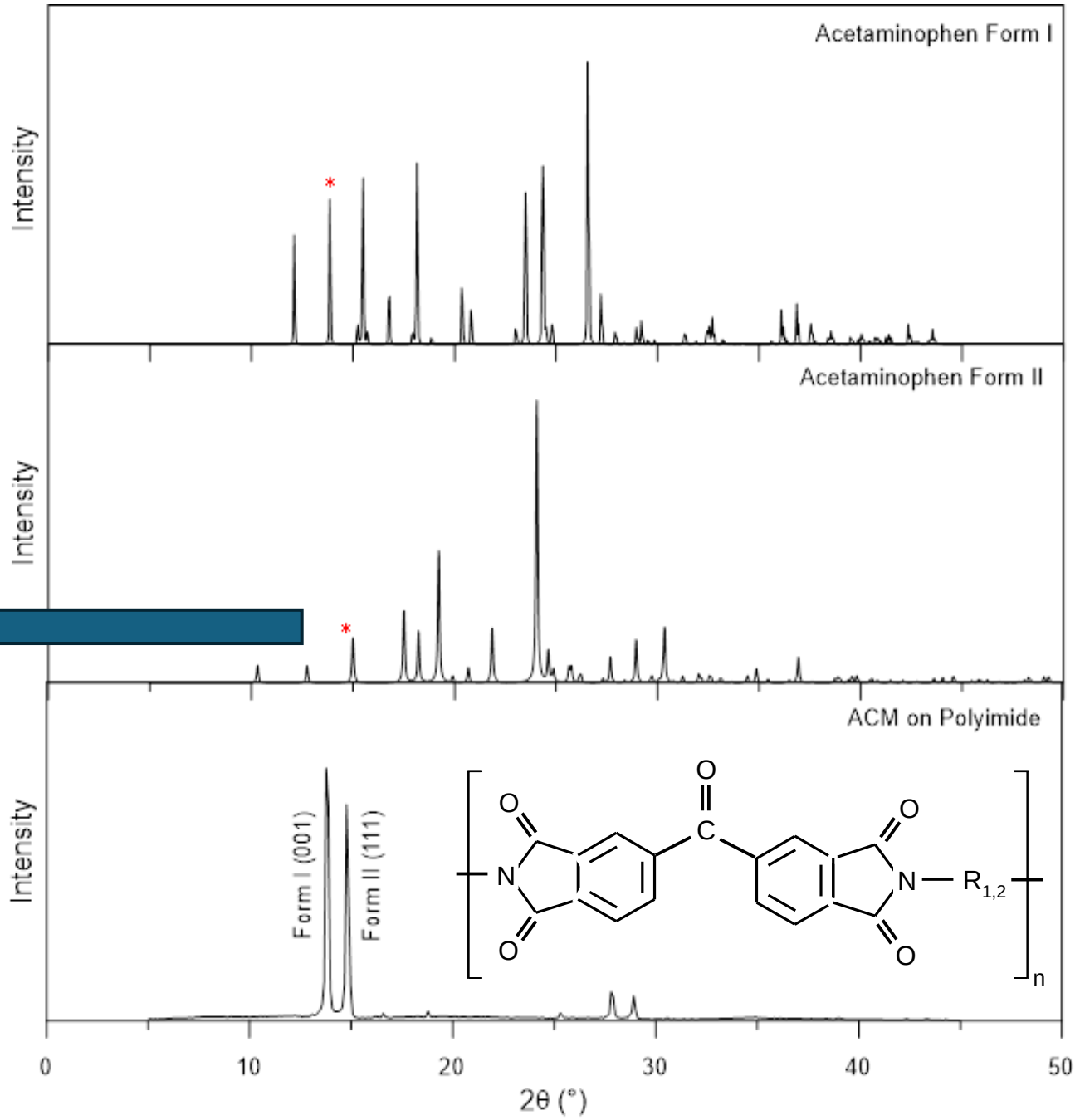

PERSPECTIVES

- New membranes: improve environmental sustainability shifting from conventional perfluorinated membranes and toxic aprotic organic solvents to biodegradable polymers and green solvent

- Energy input: integrate renewable energy sources, improve efficiency by controlling temperature polarization

- Brine treatment and resources mining: improve membrane stability in MD applications to high salinity solutions

- Broader industrial and commercial implementation to stimulate economies of scale, encourage technological advancements, and foster competitive market dynamics that make the process more accessible and cost-effective.

MEASURED

MEMBRANE SCALE-UP FOR CHEMICAL INDUSTRIES

WP3: MEMBRANES DEVELOPMENT AND SCALE-UP
TASK 3.1: DEVELOPMENT OF POLYMERIC MEMBRANES FOR MD

Funded by the European Union

Funded by the European Union under Grant Agreement No 101091887.